Review & Analysis

Vadose Zone Journal

Adsorption–Desorption Processes in Subsurface Reactive Transport Modeling

Sabine Goldberg,* Louise J. Criscenti, David R. Turner, James A. Davis, and Kirk J. Cantrell

Adsorption–desorption reactions are important processes that affect the transport of contaminants in the environment. Various empirical approaches, such as the distribution coefficient and Freundlich and Langmuir isotherm equations, have been used to represent adsorption. The empirical approaches are not capable of accounting for the effects of variable chemical conditions, such as pH, on adsorption reactions. This can be done using chemical models such as surface complexation models. These models define specific surface species, chemical reactions, equilibrium constants, mass balances, and charge balances, and their molecular features can be given thermodynamic significance. Ion adsorption mechanisms and surface configurations for the surface complexation models can be established from independent experimental observations. These include both indirect measurements, such as point of zero charge shifts, ionic strength effects, and calorimetry, and direct spectroscopic techniques, including vibrational spectroscopy, nuclear magnetic resonance (NMR) spectroscopy, and X-ray absorption spectroscopy. Surface complexation models were developed for single mineral phases but have now been applied to natural mineral assemblages using both component additivity (CA) and generalized composite (GC) approaches. Surface complexation models have been incorporated into subsurface transport models at several field sites, although simplifying assumptions are needed to deal with heterogeneous materials. Surface complexation models for contaminant adsorption have the potential to increase the confidence and scientific credibility of transport modeling by reducing the uncertainty in quantifying retardation and providing a means of quantifying that uncertainty.

Abbreviations: CA, component additivity; CCM, constant capacitance model; CD-MUSIC, charge distribution multisite complexation; CTDP, Common Thermodynamic Database Project; DLM, diffuse layer model; EXAFS, extended X-ray absorption fine structure; FTIR, Fourier transform infrared; GC, generalized composite; IR, infrared; MUSIC, multisite complexation; NEM, nonelectrostatic model; NMR, nuclear magnetic resonance; NRC, Nuclear Regulatory Commission; PZC, point of zero charge; SCM, surface complexation model; TLM, triple layer model; TPA, Total System Performance Assessment; XAS, X-ray absorption spectroscopy.

Risk assessment at contaminated field sites usually includes predictions of the fate and transport of contaminants in the vadose zone and in aquifers. Fate and transport predictions are accomplished with models that account for the physical, geochemical, and biological processes that affect future transformation and movement of the contaminants in the environment. The first step in the modeling process is the development of a conceptual model for the field site that describes the initial and boundary conditions and all of the significant processes that are occurring or that will occur in the future.

In cases where the contaminants of concern are toxic metal ions or radionuclides, the geochemical processes to be considered generally include adsorption–desorption, precipitation–dissolution, and oxidation–reduction. Studies of many contaminated field systems have demonstrated that adsorption–desorption is the most significant geochemical process affecting the transport of inorganic contaminants at specific field sites (Kent et al., 2000; Davis et al., 2004a; Kohler et al., 2004). Although laboratory adsorption–desorption equilibria in batch experiments are frequently described using surface complexation models (SCM), subsurface transport modeling of field site behavior has usually represented the adsorption process by empirical relationships, such as distribution coefficients or isotherm equations (Davis and Kent, 1990; Dzombak and Ali, 1993; USEPA, 1999b). The empirical approaches have also been used in describing retardation of metal ions in laboratory column experiments (Christensen, 1985; Buergisser et al., 1993; Hinz and Selim, 1994). As has been noted by Kent et al. (2000), the more complex SCM approach is generally not needed in cases where aqueous chemical conditions in the subsurface are temporally and spatially invariant. Examples of adsorption modeling in the field under relatively constant chemical conditions include the small-scale field experiments of Pickens et al. (1981) examining ^{90}Sr transport and the study of Cernik et al. (1994) describing zinc and copper transport in vertical soil profiles.

When adsorption is represented by empirical approaches, the conceptual model for adsorption is a simplistic one that ignores the potential impact of variable chemical conditions on adsorption (Davis and Kent, 1990). Surface complexation modeling approaches directly describe aqueous and surface speciation and distribution and therefore are capable of accounting for the effects of variable chemical conditions on adsorption.

S. Goldberg, USDA-ARS, U.S. Salinity Lab., 450 W. Big Springs Rd., Riverside, CA 92507; L.J. Criscenti, Sandia National Lab., P.O. Box 5800, MS 0750, Albuquerque, NM 87185-0750; D.R. Turner, Center for Nuclear Waste Regulatory Analyses, 6220 Culebra Rd., San Antonio, TX 78284; J.A. Davis, U.S. Geological Survey, 345 Middlefield Rd., Menlo Park, CA 94025; K.J. Cantrell, Pacific Northwest National Lab., P.O. Box 999, Richland, WA 99352. Received 30 June 2006.
*Corresponding author (sgoldberg@ussl.ars.usda.gov).

Vadose Zone J. 6:407–435
doi:10.2136/vzj2006.0085

Model calculations have provided examples of the importance of this effect on predicting the impact of adsorption (USEPA, 1999c; Bethke and Brady, 2000; Kent et al., 2000; Davis et al., 2004a). Although field-site conditions may be relatively constant in some cases, the general situations in which toxic metals are introduced into the subsurface, such as land application of sewage effluent and sludge (McBride et al., 1997), discharges from mining activities (Morin et al., 1982; Stollenwerk, 1994; Brown et al., 1998), and recharge of aquifers by contaminated surface waters (Jacobs et al., 1988; von Gunten et al., 1991), are not characterized by constant chemical conditions. Although modeling retardation is only a part of an overall risk assessment calculation for a contaminated field site, in some cases, the adsorption process may be extremely important for understanding the risk to humans (or the biosphere) or for compliance with regulations at distances far from the source of contamination. Thus, it is important that alternative conceptual models be considered in evaluating remediation approaches and risk assessments for contaminated field sites (Davis et al., 2004b). Representation of the adsorption process by empirical or SCM modeling approaches is an example of alternative conceptual models that may be needed to make predictive simulations of future behavior in contaminated field systems.

This review summarizes the current literature on adsorption–desorption reaction mechanisms, models for adsorption–desorption reactions at the molecular scale, empirical representations of adsorption–desorption equilibria, and field-scale applications of subsurface reactive transport modeling with adsorption–desorption equilibria. With the exception of the study of Vaughan et al. (2004), little information is available on the applicability of these types of modeling approaches to hydrologically unsaturated zone flow and transport, and most of the discussion is based on results documented for saturated zone flow and transport.

Conceptual Models Representing the Adsorption Process

In the literature, at least three types of conceptual models for adsorption can be distinguished: (i) empirical adsorption isotherm partitioning relationships (Davis and Kent, 1990), (ii) thermodynamic surface speciation models that describe the molecular details of chemical species formation at mineral surfaces (Hiemstra and van Riemsdijk, 1999; Sahai and Sverjensky, 1997a, 1997b); and (iii) semi-empirical site-binding models that use concepts from the first two model types to describe heterogeneous natural systems (Borkovec et al., 1998; Davis et al., 1998, 2002).

Empirical Adsorption Isotherms

Equations relating solute concentrations in coexisting solid and liquid phases can be generated for individual datasets through fitting curves and empirical coefficients to the experimental data. Empirical models have been developed to describe both equilibrium and kinetic systems. It should be noted that empirical adsorption models are applicable only for the specific conditions under which they were developed. Use of empirical models beyond these conditions could potentially lead to significant error. As a result, empirical adsorption models should be used with caution, taking care not to extend their application beyond appropriate conditions.

Linear Adsorption (K_d Approach) Isotherm

The simplest type of adsorption isotherm is a linear distribution coefficient, K_d (mL g^{-1} or m^3 kg^{-1}):

$$S = K_d C \quad [1]$$

where S (g g^{-1}) is the concentration of solute adsorbed onto the solid phase and C (g mL^{-1}) is the concentration of the solute in solution (see Fig. 1A). A linear adsorption isotherm (K_d approach) generally assumes that K_d is a constant property of an aquifer and forms the basis of the general retardation factor (R_f) through the relationship

$$R_f = 1 + \frac{\rho}{\theta} K_d \quad [2]$$

where ρ is the bulk density and θ is the porosity (Freeze and Cherry, 1979). The lower the value of K_d, the lower the retardation factor, and the faster a reactive species migrates through the subsurface. For a nonadsorbing species $K_d = 0$, R_f reduces to 1, and the species migrates at the flow velocity.

The origin of K_d as an empirical modeling parameter can be traced to descriptions of ion exchange and ion chromatography in chemical engineering practice, primarily applied to alkali and alkaline earth cations whose speciation changes little with changes in solution chemistry. Unfortunately, hydrologic modelers later assumed that this simple chemistry could be extended to essentially all inorganic contaminants and radionuclides. Perhaps the first application to transport in groundwater systems was that of Higgins (1959), who assumed that radionuclides resulting from underground nuclear explosions would adsorb via an ion exchange mechanism, with variable pH between pH 2 and 9 having a very small effect on K_d values. It has often been argued that an exact knowledge of adsorption isotherms is needed for accurate modeling of ion transport, but in the interest of computational efficiency, a constant K_d approach has been applied.

The distribution coefficient is a lumped parameter and cannot be used to represent the contributions of different uptake processes to contaminant retardation. An additional limiting

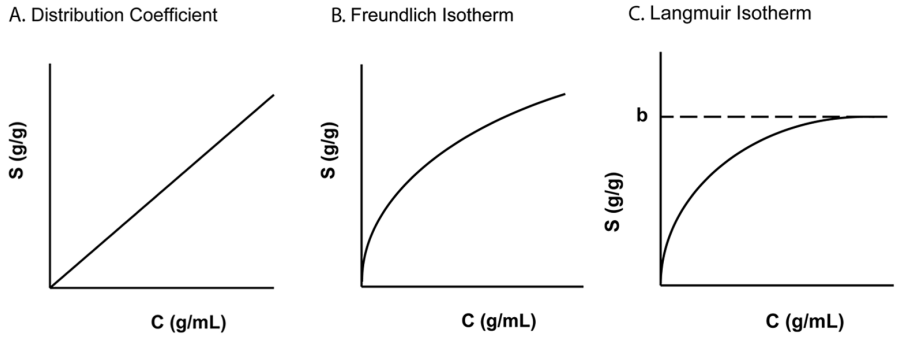

FIG. 1. Schematics depicting the form of the adsorption isotherm equations: (A) distribution coefficient, (B) Freundlich adsorption isotherm, (C) Langmuir adsorption isotherm.

characteristic of the K_d approach is its inability to recognize a maximum adsorption limit. In actuality, because there is a finite number of adsorption sites, adsorption will reach a practical upper limit.

The K_d concept works well when applied to trace concentrations of unionized, hydrophobic organic molecules. Application of this approach to inorganic contaminants, however, is problematic because the parameter is so sensitive to aqueous chemical conditions such as pH, alkalinity, or concentrations of complexing ligands that may be encountered along a groundwater flow path (Kohler et al., 1996; Davis et al., 1998, 2004a; Bethke and Brady, 2000; Kent et al., 2000; Altmann et al., 2001). For example, the K_d for uranium(VI) adsorption on ferrihydrite at pH 8 decreases by four orders of magnitude as the partial pressure of carbon dioxide gas, pCO_2, increases from its value in air (0.032%) to 1% (Davis et al., 2004a). This is an important variation to understand because the pCO_2 in aquifers commonly reaches values of 1 to 5%, whereas most K_d values have been determined in laboratory experiments equilibrated with or exposed to air. Moreover, pCO_2 often increases with transport after groundwater recharge, and this spatial–temporal trend in chemical conditions can greatly affect the retardation of contaminants. For these reasons, constant K_d models for adsorption do not adequately account for spatial variability in mineralogy and hydrochemistry along groundwater flow paths.

Freundlich Adsorption Isotherm

The Frendlich adsorption isotherm (Freundlich, 1926) is nonlinear and defined by the relationship:

$$S = K_{Fr} C^n \quad [3]$$

where S and C are defined as for Eq. [1] and K_{Fr} and n are empirical coefficients (see Fig. 1B). For the special case where $n = 1$, the Freundlich isotherm is identical to the distribution coefficient, K_d. If adsorption–concentration data can be represented by a Freundlich isotherm, a plot of log S versus log C will result in a straight line with a slope of n and an intercept of log K_{Fr}. As is the case for a linear adsorption isotherm, no adsorption maximum is reached.

Langmuir Adsorption Isotherm

In adapting the Langmuir adsorption isotherm (Langmuir, 1918) to solution chemistry, the idea of an upper limit to surface adsorption was introduced. Assuming that all adsorption sites are homogeneous, the general form of the Langmuir isotherm is

$$S = \frac{K_{La} b C}{1 + K_{La} C} \quad [4]$$

where b is the maximum adsorption capacity of the substrate (g solute g adsorbent^{-1}) and K_{La} is a constant representing the strength with which the solute is bound to the substrate (L meq^{-1}) (see Fig. 1C). Values of b and K_{La} can be determined by plotting a variety of possible linearizations or by nonlinear regression analysis (Kinniburgh, 1986).

The Langmuir isotherm accounts for the decrease in K_d values that occurs as an adsorbing surface becomes partially saturated with adsorbed species. The relationship is usually determined for a specific set of constant chemical and physical conditions and varying adsorbing ion concentration.

Parameters for Empirical Equilibrium Adsorption Models

A variety of compilations of model-dependent adsorption parameters is available in the literature. Because of its simplicity, the largest number of adsorption parameter collections is available for the distribution coefficient, K_d. In using different subsurface reactive transport computer codes, there are often default adsorption parameter values in the input files. These values may or may not be linked to experimental data or site suitable conditions, and subsequently can be revised by the user for a given simulation on a site-specific basis.

Adsorption Coefficient Databases

Due to its simplicity, the K_d approach has been applied most frequently to reactive transport, and a large amount of data is available for a number of substrates, elements, and water compositions. The Freundlich isotherm requires a value for the constant K_{Fr}, and in addition, some estimate is necessary for the empirical exponent n. As discussed above, these can be obtained from plotting log S versus log C. The Langmuir isotherm also requires two constants: K_{La}, which represents the energy of adsorption and the adsorption capacity of the substrate, b. In practice, however, experimental values for the constants neglect aqueous speciation of the solute, resulting in a simple empirical application of these isotherms.

Empirical coefficients appropriate to different models can be obtained for a given dataset by recasting the data using the adsorption–concentration expressions of the model. This can be done by curve fitting, or by plotting variables against one another on linear or logarithmic scales to determine slope and intercept values. Based on the goodness-of-fit, the more appropriate model is chosen. For systems with a large number of empirical coefficients, it is possible to have nonunique values reproduce the data equally well.

Three radiological dose assessment codes used by the U.S. Nuclear Regulatory Commission (NRC) for evaluation of decommissioning sites provide examples of K_d applications to reactive transport. These codes—DandD (Kennedy and Strenge, 1992), RESRAD (Yu et al., 1993a, 1993b), and MEPAS (Strenge and Peterson, 1989)—can be run using site-specific or default K_d values to describe adsorption. A number of other compilations of K_d values are available in the literature. These databases are not discussed in detail here. The reader should refer to the original references to locate them and then evaluate the basic assumptions and methodologies used in compiling the data.

The default K_d values used in the code DandD (Kennedy and Strenge, 1992) come from various sources or methods. If the radionuclide of interest is assumed to be mobile, a K_d value of 0.0 is assigned. Whenever possible, experimental values from Sheppard and Thibault (1990) were used. The experimental values selected from Sheppard and Thibault (1990) were the smallest of those determined from four soil types. For carbon-14 (applied as $NaH^{14}CO_3$), data from Sheppard et al. (1991) were used. When experimental data were not available, a correlation between K_d values and soil-to-plant concentration ratios was used (Thibault et al., 1990). Default K_d values used in RESRAD (Yu

et al., 1993a, 1993b) were selected from several sources available in the literature (Staley et al., 1979; U.S. Nuclear Regulatory Commission, 1980; Gee et al., 1980; Nuclear Safety Associates, 1980; Isherwood, 1981; Baes and Sharp, 1983). The default K_d values used in MEPAS (Strenge and Peterson, 1989; Whelan et al., 1996) require a value for pH and the total percentage of clay, organic matter, and iron and aluminum oxides. The list of default K_d values contains up to nine different values for each contaminant. The available K_d values are organized into three categories of pH (pH 5, pH 5–9, and pH 9). Within each pH category, the K_d values are further organized into three soil categories: the combined total percentage clay, organic matter, and iron and aluminum oxides, in three ranges (< 10%, 10–30%, and >30%).

A number of adsorption coefficient databases have been developed to address radionuclide transport issues specifically. Examples of K_d databases include the Sandia Sorption Data Management System (Siegel et al., 1989), the Atomic Energy of Canada Ltd. database (Thibault et al., 1990), the SKI Project-90 database (Andersson, 1998), and the Nuclear Energy Agency (NEA) adsorption database (Rüegger and Ticknor, 1992). Ames and Rai (1978) conducted a review of available data and relevant chemistry for radionuclide interactions with soil and rock media. Based on literature review and onsite laboratory and field experiments, Looney et al. (1987) compiled estimates of K_d values applicable to the Savannah River Site in Aiken, SC. A compilation of K_d values and supporting data applicable to the USDOE Hanford Site at Richland, WA, has been presented by Cantrell et al. (2003). Summaries of adsorption measurements (Thomas, 1987) and best estimates based on available literature (Andersson, 1998) form part of the basis for the statistical parameter distributions of radionuclide adsorption parameters in total system performance assessment analyses for the proposed high-level nuclear waste repository at Yucca Mountain, NV (Civilian Radioactive Waste Management System Management and Operating Contractor, 1998, 2000a, 2000b).

A compilation and comparison of radionuclide adsorption coefficient databases used in performance assessment have been presented by McKinley and Scholtis (1991). Although developed for the purposes of radionuclide transport, the database reviewed in their work covers nearly half of the periodic table of elements and includes information on adsorption by buffers and backfills (concrete, bentonite, clay–rock mixes), a wide range of host rocks (e.g., crystalline, sediments), and surface soils.

The USEPA has published a three-volume set of documents on understanding variation in K_d values (USEPA, 1999c, 1999d, 2002). Volume 2 (USEPA 1999d) contains a review of the geochemistry and K_d values for cadmium, cesium, chromium, lead, plutonium, radon, strontium, thorium, tritium (^{3}H), and uranium. Volume 3 (USEPA, 2002) contains a review of the geochemistry and K_d values for americium, arsenic, curium, iodine, neptunium, radium, and technetium.

Sorption coefficient databases can range from simple tabulations to probability distributions to complex interrelational computerized datasets. Historically, the tendency has been to use these databases as a source of individual adsorption coefficients for the contaminant of interest. It is important, however, that the users of these compilations understand the assumptions and experimental data (including quality assurance) that form the basis of the values presented in the database. This understanding is necessary for the user to characterize the limitations, conservatisms, and uncertainties inherent in the dataset and to make an informed decision with regard to selecting values that are appropriate for different systems. Special care should be taken in selecting adsorption coefficients for contaminants that are sensitive to geochemical conditions. For example, the value(s) selected for a redox sensitive element must be appropriate for the Eh and pH conditions likely to be encountered along the groundwater flow path.

Empirical Statistical Approaches to Predict K_ds

For any systematically generated dataset where variables that affect K_d are measured along with K_d, it is possible to use regression analyses to develop purely empirical predictor relationships. K_d is treated as the dependent variable, and the other measured variables, such as solution pH, concentration of competing ions, concentration of complexing agents, and characteristics of the adsorbent (e.g., particle size, surface area, weight percentage of specific minerals) are independent variables. Both linear and nonlinear regressions are often performed in a stepwise fashion to determine which independent variables reduce the residual error the most. The number of independent variables and the functions included in the final empirical equation are chosen based on minimization of the residual error between the measured K_d and the predicted K_d. For example, using a factorial design experimental test matrix with independent variables calcium, sodium, and potassium, Routson and Serne (1972) and Serne et al. (1974) determined the K_d for ^{90}Sr at trace levels adsorbing onto a Hanford, WA, formation sand sediment. The regression analysis resulted in a predictor equation expressing the strontium K_d as a function of the equilibrium solution concentrations of the competing cations, calcium, sodium, and potassium.

Several more recent applications of statistical analysis methods have considered implicitly the effects of chemistry on K_d values. For example, Vandergraaf et al. (1992) developed quadratic expressions to simulate radionuclide adsorption as a function of total dissolved solids and radionuclide concentration. Rosentreter et al. (1998) developed parametric K_d expressions for uranium adsorption on soil as a function of pH, surface area, and extractable iron and aluminum. Sauve et al. (2000) developed parametric expressions for a number of transition and heavy metals (cadmium, copper, nickel, lead, and zinc) presenting log K_d as a function of soil solution pH, total soil metal, and soil organic matter content. In their analysis, Sauve et al. (2000) attributed most of the variability in K_d to pH. The success of the parameterization approach in predicting K_d varied depending on the metal content.

Such statistically derived empirical functions may have some relationship to adsorption processes such as cation competition or may have little relationship to controlling processes. Because the number of variables that can influence the adsorption of a contaminant may be large in natural systems, the number of experimental parameters that should be measured and varied to develop statistical empirical functions limits the practical application of the technique. Further, many of the so-called independent variables may not truly be independent of each other, leading to the development of relationships that

have little physicochemical meaning. For example, the potential feedbacks between ambient chemistry and the changes induced by adsorption reactions (e.g., Kohler et al., 1996) are difficult to capture in this type of approach. Therefore, the statistically based empirical approach typically does not lead to a general understanding of the mechanisms controlling the interactions among soils–sediments, groundwaters–vadose zone porewaters, and contaminants.

Another drawback of these empirical conceptual models is that the calculated model parameters are not related explicitly to thermodynamic data for metal solubilities and aqueous speciation. The quality of thermodynamic data for metal solubilities and aqueous speciation has steadily increased in recent years, and the data are now available in critically reviewed compilations (Smith and Martell, 1989; Grenthe et al., 1992; Silva et al., 1995; Guillaumont et al., 2003). As will be shown below, a major advantage of the surface complexation modeling approach is that the adsorption reactions are directly related to these thermodynamic data.

Empirically Based Kinetic Adsorption Models

Kinetic adsorption models have been used to simulate conditions where adsorption processes are believed to operate relatively slowly in relation to solute residence time. For example, first-order kinetic adsorption is typically applied as a linear equation of the general form

$$\frac{dS}{dt} = k_1 - k_2 S \qquad [5]$$

where t represents time and k_1 and k_2 are rate constants for adsorption and desorption, respectively. Although k_1 and k_2 can be determined experimentally, the data are frequently unavailable and an empirical approach is used to fit Eq. [5] to adsorption data. At equilibrium, where $dS/dt = 0$, Eq. [5] reduces to the linear adsorption isotherm with $K_d = k_1/k_2$.

Different types of nonlinear reaction kinetics have also been applied to model adsorption processes using a relationship such as

$$\frac{dS}{dt} = k_1 C^n - k_2 S \qquad [6]$$

where k_1 is the adsorption (forward) rate coefficient, k_2 is the desorption (backward) rate coefficient, and n is an empirical coefficient. When $n = 1$, Eq. [6] is identical to linear kinetic adsorption described by Eq. [5]. Under equilibrium conditions, Eq. [6] reduces to the Freundlich adsorption isotherm, Eq. [3], with $K_{Fr} = k_1/k_2$.

Some adsorption experiments exhibit an initial stage of rapid, reversible adsorption followed by slow, continued irreversible uptake, and adsorption equilibrium is not reached during the duration of the experiment. In developing empirically based transport models to simulate this type of behavior, some studies proposed "two-site" models. In this empirical modeling approach, one site is assumed to achieve adsorption equilibrium rapidly, and a second "slow" adsorption site is described with a kinetic model. Several models have been used for the equilibrium site, including linear (Cameron and Klute, 1977), Freundlich (Selim et al., 1976), and Langmuir (Middleburg and Comans, 1991) isotherms. First-order reversible kinetic models have generally been applied to the "slow" site.

As in equilibrium adsorption isotherms, the required number of parameters in empirically based kinetic models varies depending on the model considered. For example, linear kinetic models require estimates of the adsorption and desorption rate constants (k_1 and k_2). Nonlinear kinetic models require estimates of these rate constants and an estimate of the empirical exponential parameter, n (see Eq. [6]). Two-site models require additional parameterization, depending on model structure. As is the case for equilibrium adsorption isotherms, experimental kinetic data are generally available for a limited number of ions and substrates, and the constants are applied as curve-fitting parameters. The application of the models depends on the underlying assumption that adsorption rates are the process-limiting factors in solute uptake. In actuality, other physical and chemical factors (e.g., pH variability, hydrologic heterogeneity) may exert some control on retardation in column and field transport experiments (Brusseau and Zachara, 1993; Painter et al., 2001). In addition, kinetic rate constants may be acquired under site-specific conditions, making extrapolation to new environments uncertain.

Surface Complexation Models

Surface complexation modeling approaches are generally more robust in application over variable geochemical conditions than empirical models because they adopt a more mechanistic approach to adsorption. This flexibility is often gained at the expense of simplicity, and SCMs may require a larger number of parameters to accommodate their increasing complexity.

Surface complexation models use mass action laws analogous to aqueous phase reactions to describe adsorption, thus accounting for changes in chemical speciation, competitive adsorption, and other multisolute interactive chemical effects (Davis and Kent, 1990; Davis, 2001). The advantages of applying the surface complexation concept to describe adsorption in risk assessment models include the following:

1. The modeling approach provides a thermodynamic framework to describe adsorption reactions of contaminants.
2. The stability constants for the adsorption reactions can be included as part of an overall network of chemical reactions in geochemical equilibrium or coupled reactive transport models and thus can be coupled with thermodynamic databases for aqueous speciation and solubilities.
3. The modeling approach allows predictive calculations for a range of chemical conditions without adjusting the values of the model parameters, as chemical conditions are varied in space or time.
4. The modeling approach can be included efficiently in transport simulations having chemical gradients in space or time.
5. The modeling approach may, in some cases, require less parameterization compared to the multiple empirical parameters necessary to capture physical and chemical heterogeneities.

Thermodynamic Surface Speciation Models

Thermodynamic surface speciation models are chemical models that provide a molecular description of adsorption phenomena using an equilibrium approach. Analogous to solution complexation, thermodynamic surface speciation models define surface species, chemical reactions, equilibrium constants, mass balances, and charge balances, and their molecular features can be given thermodynamic significance. One of the major advantages of thermodynamic surface speciation models over more empirical approaches is consideration of the charge on both the adsorbate ion and the solid adsorbent surface. Another advantage is that surface speciation models directly account for the effects of changes in aqueous speciation on the extent of the adsorption reaction. Thermodynamic surface speciation models constitute a family of models having many common chemical characteristics and adjustable parameters. The surface complexation models differ in their structural representation of the solid–solution interface, that is, the location of the adsorbing ions, and in the charge–electric potential relationships used to describe the electrostatics of the interface from the mineral surface out into bulk solution.

Surface Configuration of the Solid–Solution Interface

Members of the thermodynamic surface speciation model family include two-p*K* models: constant capacitance (Stumm et al., 1980), diffuse layer (Dzombak and Morel, 1990), and triple layer (Davis et al., 1978). Two-p*K* models contain a reactive surface functional group, SOH, which undergoes both protonation and dissociation reactions:

$$\mathrm{SOH} + \mathrm{H}^+ \rightleftarrows \mathrm{SOH}_2^+ \qquad [7]$$

$$\mathrm{SOH} \rightleftarrows \mathrm{SO}^- + \mathrm{H}^+ \qquad [8]$$

such that each has an associated equilibrium constant, hence the term, two-p*K* model (Hiemstra et al., 1989a, 1989b). Schematics of the solid–solution interface for the two-p*K* models are presented in Fig. 2A for the constant capacitance model (CCM), Fig. 2B for the diffuse layer model (DLM), and Fig. 2C for the triple layer model (TLM).

Comparable models can be written based on the one-p*K* concept in which each surface site undergoes only one protonation reaction. The one-p*K* model was developed based on the Basic Stern model. Subsequently, the multisite complexation (MUSIC) model (Hiemstra et al., 1989a, 1989b) was expanded into the charge distribution (CD)-MUSIC model using the charge distribution principle and a three-plane configuration (Hiemstra and van Riemsdijk, 1996). A schematic of the three-plane model, CD-MUSIC TPM, is presented in Fig. 2D. In the MUSIC and revised MUSIC model (Hiemstra et al., 1996), different types of surface sites are identified based on their crystallographic structure. The protonation reaction for each type of surface site may convert an unprotonated surface functional group to a protonated functional group or a protonated functional group to a doubly protonated functional group. Partial charges on each surface functional group are constrained to range from −1 to 1 and depend on the undersaturation of the surface oxygen atom (i.e., the atom is bonded to one, two, or three metal atoms within the crystal structure). In the revised MUSIC model, the partial charges also depend on the metal–oxygen bond lengths within the crystal structure. In the MUSIC model, gibbsite has only one type of surface site, which undergoes the following protonation reaction:

$$\mathrm{SOH}^{1/2-} + \mathrm{H}^+ \rightleftarrows \mathrm{SOH}_2^{1/2+} \qquad [9]$$

In the MUSIC model, protons and hydroxyls adsorb in the surface plane. The charge on these complexes and other adsorbed cations and anions is based on their corresponding charge using the bond valence principle, $s = z/\mathrm{CN}$, where s is the bond valence, z is the ion charge, and CN is the ion coordination number. In the revised MUSIC model, the bond valence s for protonated and deprotonated surface sites is based on the metal–oxygen (Me–O) distances within the crystal structure according to the expression $s = \exp[-(R - R_o)/b]$, where R is the Me–O distance, R_o is an element-specific distance, and b is a constant equal to 0.37 Å (Brown and Altermatt, 1976).

In the constant capacitance, diffuse layer, and triple layer models, the charges on the surface complexes are designated using formal charges. In the constant capacitance and diffuse layer models, all surface complexes are inner-sphere and are located in a single surface *o*-plane. The DLM also includes a "diffuse" layer where counter ions are attracted to the charged mineral surface but remain in the bulk fluid phase. In the TLM it is traditional to assign ions forming inner-sphere surface complexes to the surface *o*-plane and ions forming outer-sphere surface complexes to the outer β-plane, located between the surface plane and the diffuse layer. However, Sverjensky (2001) proposed that the TLM capacitances are correlated to the crystal-

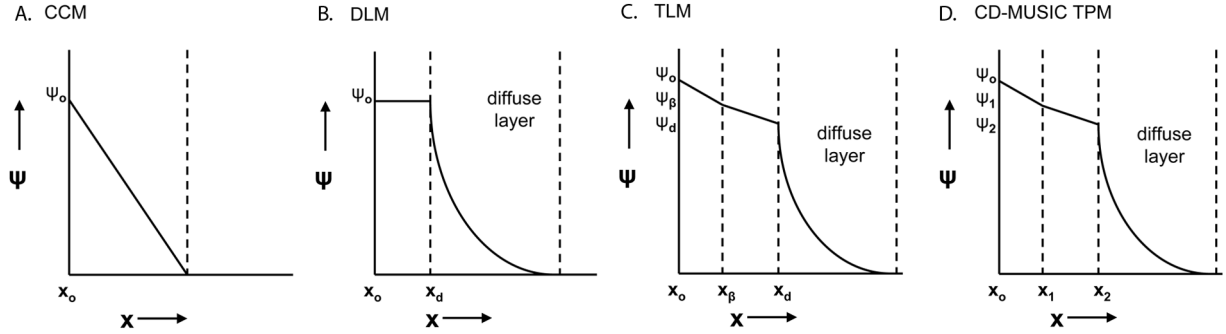

FIG. 2. Schematics depicting the solid–solution interface for the surface complexation models: (A) constant capacitance model (CCM), (B) diffuse layer model (DLM), (C) triple layer model (TLM); (D) charge distribution multisite complexation three-plane model (CD-MUSIC TPM).

lographic radius of the electrolyte cation on some minerals (i.e., rutile, anatase, and magnetite) and correlated to the hydrated electrolyte cation radius on other minerals (i.e., quartz, amorphous silica, goethite, hematite, and alumina). This would suggest that inner-sphere complexes may reside in the β-plane for minerals having high dielectric constants.

Surface Complexation Reactions

In the two-p*K* models, chemical reactions for inner-sphere surface complexation include the Eq. [7], [8], and the following:

$$\mathrm{SOH} + \mathrm{M}^{m+} \rightleftarrows \mathrm{SOM}^{(m-1)} + \mathrm{H}^{+} \quad [10]$$

$$2\mathrm{SOH} + \mathrm{M}^{m+} \rightleftarrows (\mathrm{SO})_2\mathrm{M}^{(m-2)} + 2\mathrm{H}^{+} \quad [11]$$

$$\mathrm{SOH} + \mathrm{L}^{l-} + \mathrm{H}^{+} \rightleftarrows \mathrm{SL}^{(l-1)-} + \mathrm{H_2O} \quad [12]$$

$$2\mathrm{SOH} + \mathrm{L}^{l-} + 2\mathrm{H}^{+} \rightleftarrows \mathrm{S_2L}^{(l-2)-} + 2\mathrm{H_2O} \quad [13]$$

$$\mathrm{SOH} + \mathrm{L}^{l-} + 2\mathrm{H}^{+} \rightleftarrows \mathrm{SHL}^{(l-2)-} + \mathrm{H_2O} \quad [14]$$

where M represents a metal ion of charge m^+ and L represents an anionic ligand of charge l^-. Surface complexes can be either monodentate or bidentate. Conventionally, Eq. [10–13] have been defined in the CCM. In the DLM, Eq. [14] is defined in place of Eq. [13] since bidentate complexes for adsorbed anions are not generally considered.

The following chemical reactions for outer-sphere surface complexation are defined in the TLM, in addition to Eq. [7], [8], and Eq. [10–13]:

$$\mathrm{SOH} + \mathrm{M}^{m+} \rightleftarrows \mathrm{SO}^{-} - \mathrm{M}^{m+} + \mathrm{H}^{+} \quad [15]$$

$$\mathrm{SOH} + \mathrm{M}^{m+} + \mathrm{H_2O} \rightleftarrows \mathrm{SO}^{-} - \mathrm{MOH}^{(m-1)} + 2\mathrm{H}^{+} \quad [16]$$

$$\mathrm{SOH} + \mathrm{H}^{+} + \mathrm{L}^{l-} \rightleftarrows \mathrm{SOH_2}^{+} - \mathrm{L}^{l-} \quad [17]$$

$$\mathrm{SOH} + 2\mathrm{H}^{+} + \mathrm{L}^{l-} \rightleftarrows \mathrm{SOH_2}^{+} - \mathrm{LH}^{(l-1)-} \quad [18]$$

$$\mathrm{SOH} + \mathrm{C}^{+} \rightleftarrows \mathrm{SO}^{-} - \mathrm{C}^{+} + \mathrm{H}^{+} \quad [19]$$

$$\mathrm{SOH} + \mathrm{H}^{+} + \mathrm{A}^{-} \rightleftarrows \mathrm{SOH_2}^{+} - \mathrm{A}^{-} \quad [20]$$

where C^+ is the cation and A^- is the anion of the background electrolyte.

Surface complexes for divalent metals have often been proposed to include a hydroxyl ligand (James and Healy, 1972a, 1972b, 1972c), to involve both the metal cation and the electrolyte anion (Hayes and Leckie, 1986), or to include both a metal cation and carbonate or organic acid ligands from solution in ternary surface complexes (Zachara et al., 1995). These surface complexes have been proposed within the context of both the DLM and the TLM. In the DLM, metal–anion pairs are placed in the surface plane. In the TLM, metal–anion pairs may occur on the surface *o*-plane, the β-plane, or split between the two planes. Within the context of the TLM, many different metal–anion surface complexation reactions may occur, including:

$$\mathrm{SOH} + \mathrm{M}^{2+} + \mathrm{H_2O} \rightleftarrows \mathrm{SO}^{-} - \mathrm{MOH}^{+} + 2\mathrm{H}^{+} \quad [21]$$

$$\mathrm{SOH} + \mathrm{M}^{2+} + \mathrm{H_2O} \rightleftarrows \mathrm{SOMOH} + 2\mathrm{H}^{+} \quad [22]$$

$$\mathrm{SOH} + \mathrm{M}^{2+} + \mathrm{Cl}^{-} \rightleftarrows \mathrm{SOM}^{+} - \mathrm{Cl}^{-} + \mathrm{H}^{+} \quad [23]$$

$$\mathrm{SOH} + \mathrm{M}^{2+} + \mathrm{NO_3}^{-} \rightleftarrows \mathrm{SOHM}^{2+} - \mathrm{NO_3}^{-} \quad [24]$$

In the one-p*K* models, including the CD-MUSIC model, all of these surface complexes are possible, with the added complexity that these surface complexes may occur at one or more surface site types.

Equilibrium Constants for Thermodynamic Surface Speciation Models

The following are example equilibrium constants describing inner-sphere surface complex formation in the two-p*K* models:

$$\mathrm{K}_{+} = \frac{[\mathrm{SOH_2}^{+}]}{[\mathrm{SOH}]\{\mathrm{H}^{+}\}}\exp(\mathrm{F}\psi/\mathrm{RT}) \quad [25]$$

$$\mathrm{K}_{-} = \frac{[\mathrm{SO}^{-}]\{\mathrm{H}^{+}\}}{[\mathrm{SOH}]}\exp(-\mathrm{F}\psi/\mathrm{RT}) \quad [26]$$

$${}^{1}\mathrm{K}_{\mathrm{M}} = \frac{[\mathrm{SOM}^{(m-1)}]\{\mathrm{H}^{+}\}}{[\mathrm{SOH}]\{\mathrm{M}^{m+}\}}\exp[(m-1)\mathrm{F}\psi/\mathrm{RT}] \quad [27]$$

$${}^{2}\mathrm{K}_{\mathrm{M}} = \frac{[(\mathrm{SO})_2\mathrm{M}^{(m-2)}]\{\mathrm{H}^{+}\}^2}{[\mathrm{SOH}]^2\{\mathrm{M}^{m+}\}}\exp[(m-2)\mathrm{F}\psi/\mathrm{RT}] \quad [28]$$

$${}^{1}\mathrm{K}_{\mathrm{L}} = \frac{[\mathrm{SL}^{(l-1)-}]}{[\mathrm{SOH}]\{\mathrm{L}^{l-}\}\{\mathrm{H}^{+}\}}\exp[-(l-1)\mathrm{F}\psi/\mathrm{RT}] \quad [29]$$

$${}^{2}\mathrm{K}_{\mathrm{L}} = \frac{[\mathrm{S_2L}^{(l-2)-}]}{[\mathrm{SOH}]^2\{\mathrm{L}^{l-}\}\{\mathrm{H}^{+}\}^2}\exp[-(l-2)\mathrm{F}\psi/\mathrm{RT}] \quad [30]$$

$${}^{3}\mathrm{K}_{\mathrm{L}} = \frac{[\mathrm{SHL}^{(l-2)-}]}{[\mathrm{SOH}]\{\mathrm{L}^{l-}\}\{\mathrm{H}^{+}\}^2}\exp[-(l-2)\mathrm{F}\psi/\mathrm{RT}] \quad [31]$$

where F is the Faraday constant, ψ is the surface potential, R is the molar gas constant, T is the absolute temperature, square brackets represent concentrations, and curly brackets represent activities. The exponential terms can be considered activity coefficients correcting for the effect of surface charge on surface complexation (Sposito, 1983). Equations [25–30] are conventionally considered in the CCM. In the DLM, Eq. [30] is conventionally replaced by Eq. [31]. Benjamin (2002) has shown that the mass law for formation of bidentate surface species is well represented by squaring the surface site concentration.

The following are example equilibrium constants for outer-sphere surface complex formation in the TLM:

$$^{3}K_{M} = \frac{[SO^{-} - M^{m+}]\{H^{+}\}}{[SOH]\{M^{m+}\}} \exp[F(m\psi_{\beta} - \psi_{o})/RT] \quad [32]$$

$$^{4}K_{M} = \frac{[SO^{-} - MOH^{(m-1)}]\{H^{+}\}^{2}}{[SOH]\{M^{m+}\}} \exp\left\{F\left[(m-1)\psi_{\beta} - \psi_{o}\right]/RT\right\} \quad [33]$$

$$^{4}K_{L} = \frac{[SOH_{2}^{+} - L^{l-}]}{[SOH]\{H^{+}\}\{L^{l-}\}} \exp[F(\psi_{o} - l\psi_{\beta})/RT] \quad [34]$$

$$^{5}K_{L} = \frac{[SOH_{2}^{+} - LH^{(l-1)-}]}{[SOH]\{H^{+}\}^{2}\{L^{l-}\}} \exp\left\{F\left[\psi_{o} - (l-1)\psi_{\beta}\right]/RT\right\} \quad [35]$$

$$K_{C^{+}} = \frac{[SO^{-} - C^{+}]\{H^{+}\}}{[SOH]\{C^{+}\}} \exp[F(\psi_{\beta} - \psi_{o})/RT] \quad [36]$$

$$K_{A^{-}} = \frac{[SOH_{2}^{+} - A^{-}]}{[SOH]\{H^{+}\}\{A^{-}\}} \exp[F(\psi_{o} - \psi_{\beta})/RT] \quad [37]$$

In the one-p*K* models, including the CD-MUSIC model, the equilibrium constants for surface complexation are comparable to Eq. [27–37]. For example, an equilibrium constant for surface charging of gibbsite surface sites is

$$K_{H} = \frac{[SOH_{2}^{1/2+}]}{[SOH^{1/2-}]\{H^{+}\}} \exp[F\psi_{o}/RT] \quad [38]$$

Mass and Charge Balances

Assuming that Eq. [7], [8], and [10–20] represent all the reactions occurring at the mineral surface, the mass balance for the surface functional group, SOH, in the two-p*K* models is

$$\begin{aligned} S_{T} = {} & [SOH] + [SOH_{2}^{+}] + [SO^{-}] + [SOM^{(m-1)}] \\ & + 2[(SO)_{2}M^{(m-2)}] + [SL^{(l-1)-}] \\ & + 2[S_{2}L^{(l-2)-}] + [SHL^{(l-2)-}] + [SO^{-} - M^{m+}] \\ & + [SO^{-} - MOH^{(m-1)}] \\ & + [SOH_{2}^{+} - L^{l-}] + [SOH_{2}^{+} - LH^{(l-1)-}] \\ & + [SO^{-} - C^{+}] + [SOH_{2}^{+} - A^{-}] \end{aligned} \quad [39]$$

The mass balance equations for each surface functional group (e.g., SOH, S_2OH, S_3OH, where SOH is monodentate, S_2OH is bidentate, and S_3OH is tridentate) in the one-p*K* models, including the CD-MUSIC model, are comparable. The mass balance represents a summation of all surface species for a specific site type considered in a particular thermodynamic surface speciation model.

The charge balance equations for the two-p*K* models are

$$\begin{aligned} \sigma_{o} = {} & [SOH_{2}^{+}] + [SOH_{2}^{+} - L^{l-}] + [SOH_{2}^{+} - LH^{(l-1)-}] \\ & + (m-1)[SOM^{(m-1)}] + (m-2)[(SO)_{2}M^{(m-2)}] \\ & + [SOH_{2}^{+} - A^{-}] - [SO^{-}] - [SO^{-} - M^{m+}] \\ & - [SO^{-} - MOH^{(m-1)}] - (l-1)[SL^{(l-1)-}] \\ & - (l-2)[S_{2}L^{(l-2)-}] - (l-2)[SHL^{(l-2)-}] - [SO^{-} - C^{+}] \end{aligned} \quad [40]$$

$$\begin{aligned} \sigma_{\beta} = {} & m[SO^{-} - M^{m+}] + (m-1)[SO^{-} - MOH^{(m-1)}] \\ & + [SO^{-} - C^{+}] - l[SOH_{2}^{+} - L^{l-}] \\ & - (l-1)[SOH_{2}^{+} - LH^{(l-1)-}] - [SOH_{2}^{+} - A^{-}] \end{aligned} \quad [41]$$

$$\sigma_{o} + \sigma_{d} = 0 \quad [42a]$$

$$\sigma_{o} + \sigma_{\beta} + \sigma_{d} = 0 \quad [42b]$$

where σ is the surface charge. Equations [40] and [41] represent the summation of all charge contributions in a particular adsorption plane. Equation [40] is used in all three two-pK models (CCM, DLM, and TLM), with fewer terms for the one-plane models (CCM and DLM). Equation [42a] is used in the DLM, and Eq. [41] and [42b] are used in the TLM.

The charge balance expressions for the one-p*K* models, including the CD-MUSIC model, consist of an expression similar to Eq. [42] and expressions similar to Eq. [40] and [41] for each of the planes used in the model, using partially charged surface sites. For example, for gibbsite

$$\sigma_{o} = \tfrac{1}{2}\left([SOH_{2}^{1/2+}] - [SOH^{1/2-}]\right) \quad [43]$$

Charge–Potential Relationships

All thermodynamic surface speciation models contain relationships between surface charges and surface potentials. In the CCM, the charge-potential relation is

$$\sigma = C\psi \quad [44]$$

where C is the capacitance. The charge–potential relation for a symmetrical electrolyte in the DLM is

$$\sigma_{d} = -\left(8\varepsilon_{o}DRTI\right)^{1/2} \sinh(F\psi_{d}/2RT) \quad [45]$$

where ε_o is the permittivity of vacuum, *D* is the dielectric constant of water, and *I* is the solution ionic strength. In the TLM the charge-potential relations are Eq. [45] and

$$\sigma_{o} = C_{1}\left(\psi_{o} - \psi_{\beta}\right) \quad [46]$$

$$\sigma_{d} = C_{2}\left(\psi_{d} - \psi_{\beta}\right) \quad [47]$$

Establishing Ion Adsorption Mechanisms

In using thermodynamic surface speciation models, the user must select the appropriate surface complexes that specify the adsorption mechanisms for all adsorbing ions. Inner-sphere surface complexes contain no water between the adsorbate ion and the mineral surface functional groups, while outer-sphere surface complexes contain at least one water molecule between the adsorbate ion and the surface. The CCM and the DLM consider all adsorbing ions to form inner-sphere complexes. In the TLM and the CD-MUSIC model, the mechanism of ion adsorption can be either inner-sphere or outer-sphere. To preserve the chemical

significance of thermodynamic surface speciation models, ion adsorption mechanisms should be established from independent experimental observations. Indirect experimental procedures that also provide guidance about ion adsorption mechanisms include point of zero charge shifts, ionic strength dependence, and calorimetry.

Spectroscopic Techniques

The structures of surface complexes and oxide surfaces have been studied using a variety of spectroscopic and scattering techniques, including X-ray absorption spectroscopy (XAS), X-ray standing wave spectroscopy, infrared (IR) spectroscopy, second-harmonic generation, X-ray diffraction, and X-ray reflectivity (Brown et al., 1989). No single technique can provide a complete description of the surface or of the surface species. Several of these methods are summarized below, along with examples of the types of data derived from each method. Table 1 provides a list of spectroscopic studies of surface speciation for different elements of concern.

Infrared Spectroscopy

Infrared spectroscopy has proven to be a useful technique for studying the interactions of ions with surfaces. Direct evidence for inner-sphere surface complexation of anions via ligand exchange has come from IR spectroscopic characterization using both dispersion IR and Fourier transform infrared (FTIR) spectrometers. One of the advantages of FTIR is that water peaks can be subtracted mathematically, allowing analyses of more realistic wet systems, unlike dispersion IR, which must be performed in a vacuum. Artifacts can be produced when extrapolating results from evacuated samples to aqueous solutions. For example, results from evacuated systems showed a predominance of bidentate surface complexes for most anions. However, the addition of water to bidentate surface complexes will drive the equilibrium to favor the formation of monodentate surface complexes.

Manning and Goldberg (1996) postulated a mixture of bidentate and monodentate surface complexes in modeling phosphate adsorption on goethite with the CCM, consistent with FTIR results. Raman and FTIR spectroscopic studies of arsenic adsorption indicated inner-sphere surface complexes for arsenate on amorphous iron and aluminum oxide and arsenite on amorphous iron oxide and outer-sphere surface complexes for arsenite on amorphous aluminum oxide (Goldberg and Johnston, 2001). These surface configurations were used to constrain the surface complexes in the application of the CCM and the TLM to describe the arsenic adsorption data (Goldberg and Johnston, 2001). Villalobos and Leckie (2001) used their FTIR spectroscopic results to successfully describe carbonate adsorption on goethite using the TLM.

Nuclear Magnetic Resonance Spectroscopy

Nuclear magnetic resonance spectroscopic experiments can distinguish between protonated and unprotonated surface complexes and between inner- and outer-sphere surface complexes. Bleam et al. (1991) found NMR signals that exhibited significant spinning side band intensity and ready cross-polarization, indicative of phosphate adsorbed onto a boehmite surface as an inner-sphere complex. Interrupted decoupling $^{31}P\{^{1}H\}$ cross-polarization, magic-angle-spinning NMR experiments discriminated between protonated and deprotonated surface species and indicated that surface adsorbed phosphate became deprotonated in the pH range 9 to 11. This pH range agreed with that predicted by Goldberg and Sposito (1984) for various aluminum oxides and by Bleam et al. (1991) for boehmite using the CCM. Similar approaches can be used to study ^{29}Si, ^{11}B, and ^{75}As adsorption on aluminum oxides.

X-Ray Absorption Spectroscopy

X-ray absorption spectroscopy is useful for determining many of the structural details of adsorbed species (Koretsky, 2000; Brown, 1990; Greaves, 1995; Brown et al., 1995; Brown et al., 1989). Two types of spectra are produced with this technique: X-ray absorption near edge structure and extended X-ray absorption fine structure (EXAFS). X-ray absorption near edge structure spectra provide quantitative information on the oxidation state of an absorbing element and its coordination number. Extended X-ray absorption fine structure spectra provide information including the average distance to, and the number and identity of atoms, in the first and second coordination shells (∼6 Å radius) around a metal ion. This information is used to determine whether the ion is adsorbed to the surface as an inner-sphere or outer-sphere complex, as a monodentate, bidentate, or tridentate complex, and as a mononuclear complex, multinuclear complex, or as a precipitate (see Fig. 3). Extended X-ray absorption fine structure spectra are capable of yielding average interatomic distances accurate to better than ± 0.02 Å and average coordination numbers accurate to ±15 to 20%. It is important to recognize that this structural information is summed over all of the environments of a given element. These environments will not be distinguishable in the EXAFS spectrum unless the average *M–O* distance differs by ≥0.1 Å between different surface sites on an oxide or silicate mineral. Octahedral and tetrahedral site geometries can usually be distinguished (Brown et al., 1995).

Sorption samples suitable for in situ XAS experiments may be of two forms: wet, high surface area (<1 to >100 $m^2\ g^{-1}$) powdered solids or flat single crystal surfaces on which a particular type of cation or oxyanion is adsorbed. The wet, powdered sample is typically in the form of a paste with a volume between a few μm^3 to 1 cm^3. Surface coverages range from very low (<0.1 monolayer of adsorbate ion) to greater than one monolayer on both high surface area powders and oriented single crystals for a variety of adsorbate–adsorbent systems.

Table 1 provides a list of spectroscopic studies investigating the structure of adsorbing cations and anions on oxides and clay minerals with brief summaries of the data interpretation. It should be noted that, in several cases, studies that at first glance appear to be identical (i.e., the same adsorbate and same adsorbent) may give different results. For example, Manceau and Charlet (1994) found that selenate (SeO_4^{2-}) adsorbed to goethite as an inner-sphere complex, while Hayes et al. (1987) found that SeO_4^{2-} adsorbed to goethite as an outer-sphere complex. Later, Peak and Sparks (2002) did a more comprehensive study of selenate adsorption onto goethite over a wider range of pH, ionic strength, and surface coverage. They found that selenate adsorbed as an inner-sphere complex at pH 3.5 and an outer-sphere complex at pH 6. In addition, at a pH of 3.5, selenate adsorption changed from outer-sphere to inner-sphere with increasing ionic strength. Amorphous hydroxides differ in

TABLE 1. Summary of spectroscopic information to support speciation at the mineral–water interface.

Adsorbed species	Solid	Spectroscopic method†	Adsorption mechanism	Reference
Pb^{2+}	Quartz	XAS	Inner-sphere; polynuclear complexes at higher surface coverages	Chen et al. (2006)
Pb^{2+}	γ-Al_2O_3	XAS	Inner-sphere, monodentate; possibly some multinuclear at higher surface coverages	Chisholm-Brause et al. (1990a)
Pb^{2+}	Al_2O_3 powders α-Al_2O_3 and γ-Al_2O_3	XAS	Mononuclear bidentate complexes to edges of AlO_6 octahedra; dimeric complexes at higher surface coverages	Bargar et al. (1997a)
Pb^{2+}	γ-Al_2O_3	XAS	Inner-sphere bidentate edge	Strawn et al. (1998)
Pb^{2+}	γ- Al_2O_3	XAS	Mononuclear bidentate complexes to edges of AlO_6 octahedra	Bargar et al. (1998)
Pb^{2+}	Boehmite	XAS	Pb-O clusters form	Weesner and Bleam (1998)
Pb^{2+}	α-Al_2O_3 (1 $\bar{1}$ 02) and (0001)	GI-XAFS	Inner-sphere on (1 $\bar{1}$ 02); outer-sphere on (0001)	Bargar et al. (1996, 1997c)
Pb^{2+}	Goethite	XAS	Mononuclear bidentate complexes to edges of FeO_6	Bargar et al. (1997b)
Pb^{2+}	Goethite	XAS	Inner-sphere	Weesner and Bleam (1998)
Pb^{2+}	Goethite	XAS	Pb-Cl ternary complexes with both inner-sphere Pb and Cl; bidentate inner-sphere Pb surface complexes	Bargar et al. (1998)
Pb^{2+}	Hematite	XAS	Mononuclear bidentate complexes to edges of FeO_6	Bargar et al. (1997b)
Pb^{2+}	Hydrous ferric oxide	XAS	Inner-sphere monodentate and bidentate	Trivedi et al. (2003)
Pb^{2+}	Montmorillonite	XAS	Outer-sphere, probably on basal planes; inner-sphere, probably on clay edges	Strawn and Sparks (1999)
Cd^{2+}	Goethite	XAS	Inner-sphere bidentate at corner-sharing sites on predominant (110) crystal surface	Randall et al. (1999)
Cd^{2+}	Lepidocrocite	XAS	Inner-sphere bidentate and/or tridentate edge-sharing sites	Randall et al. (1999)
Cd^{2+}	Akageaneite	XAS	Inner-sphere	Randall et al. (1999)
Cd^{2+}	Schwertmannite	XAS	Inner-sphere	Randall et al. (1999)
Cd^{2+}	Lepidocrocite	XAS	Edge-sharing, inner-sphere	Manceau et al. (2000)
Co^{2+}	Quartz	XAS	Large, multinuclear complexes or disordered hydroxide-like precipitates	O'Day et al. (1996)
Co^{2+}	Silica	XAS	Formation of solid phase, Co–kerolite	Chen et al. (2006)
Co^{2+}	γ-Al_2O_3	XAS	Inner-sphere, multinuclear	Chisholm-Brause et al. (1990b)
Co^{2+}	γ-Al_2O_3	XAS	Coprecipitates consistent with Co(II)–Al(III) layered double hydroxides	Boyle-Wight et al. (2002)
Co^{2+}	90% α-Al_2O_3/10% γ-Al_2O_3	XAS	Small multinuclear complexes at low adsorption densities; disordered, hydrous, surface-induced precipitate at highest adsorption densities.	Towle et al. (1997a, b)
Co^{2+}	α-Al_2O_3 (1 $\bar{1}$ 02) and (0001)	GI-XAFS	Inner-sphere, mostly tridentate on (0001) and tetradentate on (1 $\bar{1}$ 02)	Towle et al. (1999a)
Co^{2+}	α-Al_2O_3	XAS	Inner-sphere, surface precipitation at high surface coverage	Hayes and Katz (1996)
Co^{2+}	Rutile	XAS	Inner-sphere, multinuclear	Chisholm-Brause et al. (1990b)
Co^{2+}	Rutile	XAS	Low surface coverage: mononuclear or small multinuclear; high surface coverage: large multinuclear complexes with anatase-like structure	O'Day et al. (1996)
Co^{2+}	TiO_2 (rutile) (110) and (001)	GI-XAFS	Inner-sphere, bidentate or tetradentate on (001), monodentate or bidentate to (110)	Towle et al. (1999b)
Co^{2+}	Kaolinite	XAS	Inner-sphere, multinuclear	Chisholm-Brause et al. (1990b)
Co^{2+}	Kaolinite	XAS	Oxide or hydroxide-bridged multinuclear complexes at low surface coverage and higher surface coverages	O'Day et al. (1994a)
Co^{2+}	Kaolinite	XAS	At low surface coverage bidentate, inner-sphere, mononuclear complexes form; at >5% surface coverage, multinuclear complexes form	O'Day et al. (1994b)
Co^{2+}	Kaolinite	XAS	Adsorption of hydroxyl-bridged Co polymers or Co and Al multimers; precipitation of cobalt hydrotalcite at higher surface coverage	Thompson et al. (1999)
Co^{2+}	Kaolinite	XAS	Outer-sphere mononuclear complexes at permanent charge sites; at high pH, Co coprecipitates	Chen and Hayes (1999)
Co^{2+}	Illite	XAS	Outer-sphere mononuclear complexes at permanent charge sites; at high pH, Co coprecipitates	Chen and Hayes (1999)
Co^{2+}	Hectorite	XAS	Outer-sphere mononuclear complexes at permanent charge sites; at high pH, Co coprecipitates	Chen and Hayes (1999)
Co^{2+}	Montmorillonite	XAS	Outer-sphere mononuclear complexes at permanent charge sites; at high pH, Co coprecipitates	Chen and Hayes (1999)
Cu^{2+}	Amorphous silica	XAS	Dimeric Cu(II) complex dominates, with a minority of monomeric Cu(II) complex; inner-sphere, monodentate; aging increases ratio of dimeric:monomeric	Cheah et al. (1998)
Cu^{2+}	γ-Al_2O_3	XAS	Monomeric species, inner-sphere monodentate or bidentate	Cheah et al. (1998)
Cu^{2+}	Boehmite	XAS	Inner-sphere, low surface coverage; $Cu(OH)_N(H_2O)_x^{(2-N)+}$ outer-sphere, high surface coverage	Weesner and Bleam (1997)
Hg^{2+}	Goethite	XAS	Inner-sphere, bidentate to edge-sharing sites on (110) surface	Collins et al. (1999)
Zn^{2+}	α-Al_2O_3 and γ-Al_2O_3	XAS	Inner-sphere, bidentate at low surface coverages, formation of mixed Zn–Al hydroxide coprecipitate at high surface coverages	Trainor et al. (2000)
Zn^{2+}	Hydrous ferric oxide	XAS	Inner-sphere, bidentate at low surface coverages, coprecipitate at higher surface coverages	Waychunas et al. (2002, 2003)
Zn^{2+}	Hydrous ferric oxide	XAS	Outer-sphere	Trivedi et al. (2001a)
Zn^{2+}	Goethite	XAS	Inner-sphere, bidentate	Trivedi et al. (2001a)
Zn^{2+}	Hydrous manganese oxide	XAS	Outer-sphere	Trivedi et al. (2001b)
UO_2^{2+}	Amorphous silica	XAS	Inner-sphere, bidentate at low pH, polynuclear at near-neutral pH	Sylwester et al. (2000)
UO_2^{2+}	γ-Al_2O_3	XAS	Inner-sphere, bidentate at low pH, polynuclear at near-neutral pH	Sylwester et al. (2000)
UO_2^{2+}	Goethite	XAS	Inner-sphere, bidentate	Moyes et al. (2000)
UO_2^{2+}	Lepidocrocite	XAS	Inner-sphere, bidentate	Moyes et al. (2000)
UO_2^{2+}	hematite	XAS	Inner-sphere bidentate uranyl-carbonate complexes. Monomeric below pH 5, dimeric above pH 6.5	Bargar et al. (2000)
UO_2^{2+}	Hydrous ferric oxide	XAS	Inner-sphere, mononuclear, bidentate complex; bidentate, ternary UO_2CO_3 complex at alkaline pH	Waite et al. (1994)
UO_2^{2+}	Imogolite	XAS	Inner-sphere, bidentate and uranyl-biscarbonato complexes at low pH; outer-sphere uranyl-triscarbonato at high pH	Arai et al. (2006)
UO_2^{2+}	Muscovite	XAS	Surface precipitation	Moyes et al. (2000)
UO_2^{2+}	Montmorillonite	XAS	Ion-exchange at low pH; inner-sphere at near-neutral pH	Sylwester et al. (2000)

TABLE 1. Continued..

Adsorbed species	Solid	Spectroscopic method†	Adsorption mechanism	Reference
UO_2^{2+}	Montmorillonite	Emission	Exchange, inner-sphere, polymeric, maybe outer-sphere	Chisholm-Brause et al. (2001)
UO_2^{2+}	Mackinawite (iron sulfide)	XAS	Inner-sphere, bidentate at low surface coverage; partial reduction of uranium at higher surface coverages	Moyes et al. (2000)
Ni^{2+}	Silica	XAS	Surface precipitate, α-type metal hydroxides	Scheinost and Sparks (2000)
Ni^{2+}	Gibbsite	XAS	Multinuclear surface complexes, takovite-like; mixed Ni/Al phase at 0.1 μmol m^{-2}	Scheidegger et al. (1997, 1998)
Ni^{2+}	Gibbsite	XAS	Surface precipitate, layered double hydroxide above pH 7	Scheinost and Sparks (2000)
Ni^{2+}	Kaolinite	XAS	Multinuclear surface complexes, takovite-like	Scheidegger et al. (1997)
Ni^{2+}	Pyrophyllite	XAS	Multinuclear surface complexes, takovite-like bond lengths; mixed Ni/Al phase at 0.7 μmol m^{-2}	Scheidegger et al. (1996, 1997, 1998)
Ni^{2+}	Pyrophyllite	XAS	Surface precipitate, layered double hydroxide above pH 7	Scheinost and Sparks (2000)
Ni^{2+}	Montmorillonite	XAS	Multinuclear surface complexes, takovite-like; mixed Ni/Al phase at 0.19 μmol/m^{-2}	Scheidegger et al. (1997, 1998)
Ni^{2+}	Montmorillonite	XAS	Inner-sphere, mononuclear on edges	Dähn et al. (2003)
Ni^{2+}	Talc	XAS	Surface precipitate, α-type metal hydroxides	Scheinost and Sparks (2000)
Ni^{2+}	Hydrous manganese oxide	XAS	Outer-sphere	Trivedi et al. (2001b)
Sr^{2+}	Silica	XAS	Outer-sphere	Chen et al. (2006)
Sr^{2+}	Goethite	XAS	Inner-sphere	Collins et al. (1998)
Sr^{2+}	Amorphous silica	XAS	Outer-sphere	Sahai et al. (2000)
Sr^{2+}	Goethite	XAS	Outer-sphere	Sahai et al. (2000)
Sr^{2+}	Kaolinite	XAS	Outer-sphere	Sahai et al. (2000)
Sr^{2+}	Kaolinite	XAS	Mononuclear, outer-sphere	Chen et al. (1998); Chen and Hayes (1999)
Sr^{2+}	Illite	XAS	Mononuclear, outer-sphere	Chen et al. (1998); Chen and Hayes (1999)
Sr^{2+}	Hectorite	XAS	Mononuclear, outer-sphere	Chen et al. (1998); Chen and Hayes (1999)
Sr^{2+}	Montmorillonite	XAS	Mononuclear, outer-sphere	Chen et al. (1998); Chen and Hayes (1999)
Cs^{+}	Vermiculite	XAS	Inner- and outer-sphere	Bostick et al. (2002)
Cs^{+}	Montmorillonite	XAS	Inner- and outer-sphere	Bostick et al. (2002)
CrO_4^{2-}	Silica	XAS	Monodentate surface complex and surface nucleated chromium oxyhydroxide	Fendorf et al. (1994)
CrO_4^{2-}	Goethite	XAS	Monodentate at low surface coverage; bidentate at high surface coverage	Fendorf et al. (1997)
CrO_4^{2-}	Hydrous ferric oxide	XAS/FTIR	Inner-sphere	Hsia et al. (1993)
AsO_4^{3-}	Gibbsite	XAS	Inner-sphere, bidentate–binuclear	Ladeira et al. (2001)
AsO_4^{3-}	Amorphous Al oxide	Raman/FTIR	Inner-sphere	Goldberg and Johnston (2001)
AsO_4^{3-}	γ-Al_2O_3	XAS	Inner-sphere, bidentate–binuclear	Arai et al. (2001)
AsO_4^{3-}	Goethite	XAS	Monodentate at low surface coverage; bidentate at high surface coverage	Fendorf et al. (1997)
AsO_4^{3-}	Goethite	XAS	Inner-sphere bidentate	Waychunas et al. (1993)
AsO_4^{3-}	Hematite	XAS	Inner-sphere, bidentate mononuclear and bidentate binuclear	Arai et al. (2004)
AsO_4^{3-}	Hydrous ferric oxide	XAS	Monodentate, inner-sphere bidentate	Waychunas et al. (1993)
AsO_4^{3-}	Hydrous ferric oxide	FTIR	Inner-sphere	Hsia et al. (1994)
AsO_4^{3-}	Hydrous ferric oxide	Raman/FTIR	Inner-sphere and outer-sphere	Goldberg and Johnston (2001)
AsO_4^{3-}	Akaganeite	XAS	Inner-sphere bidentate	Waychunas et al. (1993)
AsO_4^{3-}	Lepidocrocite	XAS	Inner-sphere bidentate	Waychunas et al. (1993)
AsO_4^{3-}	Allophane	XAS	Inner-sphere, bidentate-binuclear	Arai et al. (2005)
AsO_3^{3-}	Amorphous Al oxide	Raman/FTIR	Outer-sphere	Goldberg and Johnston (2001)
AsO_3^{3-}	γ-Al_2O_3	XAS	Inner-sphere bidentate–binuclear and outer-sphere	Arai et al. (2001)
AsO_3^{3-}	Hydrous ferric oxide	Raman/FTIR	Inner- and outer-sphere	Goldberg and Johnston (2001)
SeO_4^{2-}	γ-Al_2O_3	FTIR	Inner- and outer-sphere	Wijnja and Schulthess (2000)
SeO_4^{2-}	Goethite	XAS	Outer-sphere	Hayes et al. (1987)
SeO_4^{2-}	Goethite	XAS	Inner-sphere, bidentate–binuclear	Manceau and Charlet (1994)
SeO_4^{2-}	Goethite	XAS	Inner- and outer-sphere	Peak and Sparks (2002)
SeO_4^{2-}	Goethite	FTIR	Inner- and outer-sphere	Wijnja and Schulthess (2000)
SeO_4^{2-}	Hematite	XAS	Inner-sphere	Peak and Sparks (2002)
SeO_4^{2-}	Hydrous ferric oxide	XAS	Inner-sphere	Peak and Sparks (2002)
SeO_4^{2-}	Hydrous ferric oxide	XAS	Inner-sphere, bidentate–binuclear	Manceau and Charlet (1994)
SeO_4^{2-}	Hydrous ferric oxide	FTIR	Inner-sphere	Su and Suarez (2000)
SeO_3^{2-}	Goethite	XAS	Inner-sphere, bidentate	Hayes et al. (1987)
SeO_3^{2-}	Hydrous ferric oxide	FTIR	Inner-sphere	Su and Suarez (2000)
PO_4^{3-}	Pseudoboehmite	NMR	Inner-sphere	Bleam et al. (1991)
PO_4^{3-}	Goethite	FTIR	Protonated–nonprotonated bridging bidentate; nonprotonated bridging monodentate	Tejedor-Tejedor and Anderson (1990)
PO_4^{3-}	Goethite	FTIR	Monodentate	Persson et al. (1996)
$B(OH)_4^{-}$	Hydrous ferric oxide	FTIR	Inner-sphere	Su and Suarez (1995)
CO_3^{2-}	γ-Al_2O_3	FTIR	Inner-sphere, monodentate	Wijnja and Schulthess (1999)
CO_3^{2-}	Amorphous Al oxide	FTIR	Inner-sphere, monodentate	Su and Suarez (1997)
CO_3^{2-}	Gibbsite	FTIR	Probably inner-sphere, monodentate	Su and Suarez (1997)
CO_3^{2-}	Hydrous ferric oxide	FTIR	Inner-sphere, bicarbonate and carbonate	Su and Suarez (1997, 2000)
CO_3^{2-}	Goethite	FTIR	Inner-sphere, monodentate	Su and Suarez (1997); Villalobos and Leckie (2001); Wijnja and Schulthess (2001)
SO_4^{2-}	γ-Al_2O_3	FTIR	Inner- and outer-sphere	Wijnja and Schulthess (2000)
SO_4^{2-}	Goethite	FTIR	Inner- and outer-sphere	Peak et al. (1999); Wijnja and Schulthess (2000)
SO_4^{2-}	Hydrous ferric oxide	FTIR	Inner-sphere	Hug (1997)

† FTIR, Fourier transform infrared; GI-XAFS, grazing incidence–X-ray absorption fine structure; NMR, nuclear magnetic resonance; XAS, X-ray absorption spectroscopy.

composition based on the method used to make them in the laboratory and as a function of aging (Goldberg et al., 2001). The adsorption properties and the spectroscopic results regarding the structure of adsorbed species on these naturally ubiquitous materials can vary accordingly. Discrepancies between spectroscopic results from different studies can also be attributed to differences in reaction conditions (e.g., solution pH, ionic strength, solid concentration).

X-ray absorption spectroscopic techniques for studying metal adsorption to oxides from aqueous solution are continuously being refined. Therefore, more recent spectroscopic studies may disagree with previous ones because they use an updated approach. For example, O'Day et al. (2000) did detailed EXAFS analyses on strontium in different compounds and in solution to quantify local thermal and static disorder and to characterize strontium coordination in a variety of oxygen-ligated bonding environments. These authors concluded that previous spectroscopic determinations of hydrated strontium may have underestimated first-shell interatomic distances and coordination numbers.

The results from spectroscopic studies provide information on the stoichiometry and structure of surface complexes that is being used to constrain the reactions considered when applying SCMs to bulk adsorption data. Katz and Hayes (1995) proposed a continuum thermodynamic surface speciation model consistent with spectroscopic observations (Chisholm-Brause et al., 1990b) for changing cobalt surface coverage on alumina surfaces. Manning and Goldberg (1996) postulated a mixture of bidentate and monodentate surface complexes in modeling arsenate adsorption on goethite with the CCM, consistent with the results of Waychunas et al. (1993). Using EXAFS, Manning et al. (1998) observed a bidentate, binuclear bridging surface complex for arsenite on goethite. This surface complex was incorporated into the CCM and an excellent fit of arsenite adsorption data was obtained. Venema et al. (1996) successfully described cadmium adsorption on goethite with the CD-MUSIC model using the surface species observed in the EXAFS study of Spadini et al. (1994). Grossl et al. (1997) used the EXAFS results of Fendorf et al. (1997) to successfully describe arsenate and chromate adsorption on goethite using the CCM. Dyer et al. (2003) were able to describe lead adsorption on amorphous iron oxide with the TLM using the bidentate mononuclear and monodentate mononuclear surface species observed in the XAS study of Trivedi et al. (2003).

Indirect Measurements

Point of Zero Charge Shifts

The point of zero charge (PZC) of a solid phase can be measured indirectly electrokinetically, in colloidal stability experiments, or from potentiometric titrations. Electrophoretic mobility is a measure of the movement of charged particles in an electric field where zero electrophoretic mobility indicates zero net surface charge, the isoelectric point. Specific inner-sphere ion adsorption produces shifts in PZC and reversals of electrophoretic mobility with increasing concentration of the ion (Hunter, 1981). Shifts in PZC have been observed with phosphate (Anderson and Malotky, 1979), arsenate (Anderson et al., 1976; Harrison and Berkheiser, 1982; Suarez et al., 1999),

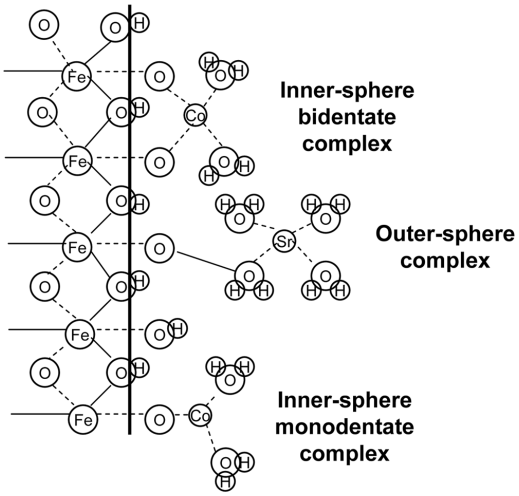

FIG. 3. Schematic indicating the formation of inner-sphere and outer-sphere complexes at the solid–solution interface. After Hayes and Katz (1996).

arsenite (Pierce and Moore, 1980; Suarez et al., 1999), chromate (Lumsdon et al., 1984), carbonate (Su and Suarez, 1997), selenite, selenate (Su and Suarez, 2000), molybdate (McKenzie, 1983; Goldberg et al., 1996), and borate (Goldberg et al., 1993; Su and Suarez, 1995) adsorption on oxide minerals. Consistent with their electrophoretic mobility results, Goldberg et al. (1993) postulated an inner-sphere surface complex to model borate adsorption on oxides and clay minerals. Adsorption that results in shifts in PZC indicates that forces in addition to electrostatic attraction are involved in the adsorption mechanism. Typically this means that inner-sphere complexes are formed, although outer-sphere complexes bound by strong hydrogen bonds cannot be ruled out. Adsorption that does not result in a shift in PZC may be due to either inner-sphere or outer-sphere surface complex formation.

Ionic Strength Effects

Use of ionic strength dependence of adsorption to distinguish indirectly between inner- and outer-sphere surface complexes has been advocated for metal ions (Hayes and Leckie, 1987) and anions (Hayes et al., 1988). Ions showing little ionic strength dependence in their adsorption behavior, such as lead, cadmium (Hayes and Leckie, 1987), selenite (Hayes et al., 1988), borate (Goldberg et al., 1993), and arsenate (Hsia et al., 1994; Goldberg and Johnston, 2001), are considered specifically adsorbed as strong inner-sphere surface complexes. Ions showing strong ionic strength dependence in their adsorption behavior, such as selenate (Hayes et al., 1988), are considered to be weakly bound as outer-sphere surface complexes, although ionic strength dependence could also indicate that a mixture of inner-sphere and outer-sphere complexes is formed.

McBride (1997) refined this concept, indicating that ions that show decreasing adsorption with increasing ionic strength are adsorbed as outer-sphere surface complexes, while ions that show little ionic strength dependence or show increasing adsorption with increasing ionic strength are adsorbed as inner-sphere surface complexes. Greater adsorption with increasing ionic strength results from the higher activity of counter ions available in solution to compensate for the surface charge generated by specific ion adsorption. Criscenti and Sverjensky (1999) showed

that transition and heavy metals that were thought to not exhibit ionic strength dependence in adsorption behavior in fact exhibited a dependence that was a function of the background electrolyte in solution. In $NaNO_3$ solutions, these ions exhibited no ionic strength dependence in their adsorption behavior; in NaCl solutions, they consistently exhibited decreasing adsorption with increasing ionic strength; and in $NaClO_4$ solutions, they exhibited an increase in adsorption with increasing ionic strength.

The inner-sphere adsorption mechanism for selenite and the outer-sphere adsorption mechanism for selenate deduced from ionic strength dependence was verified using EXAFS spectroscopy (Hayes et al., 1987). However, in disagreement with the data of Hayes et al. (1987), Manceau and Charlet (1994), using EXAFS spectroscopy, observed selenate forming inner-sphere surface complexes on goethite and hydrous iron oxide and questioned the relevance of ionic strength dependence data as a criterion for formation of outer-sphere surface complexes. For divalent cations, transition and heavy metal adsorption can still, in general, be described by inner-sphere complexes; for alkaline earth metals, adsorption can be described by outer-sphere surface complexes, as proposed by Hayes and Leckie (1987). However, this generalization may be less applicable as more experiments are conducted in electrolyte solutions other than $NaNO_3$.

Calorimetry

By measuring the heat change resulting from adsorption reactions, titration calorimetry can provide useful information on the strength of adsorbate–adsorbent interactions (Zeltner et al., 1986). This information provides indirect evidence for possible adsorption mechanisms. Titration calorimetry suggested that salicylate was adsorbed as a bidentate complex on goethite (Zeltner et al., 1986). Adsorption enthalpies determined for fluoride, iodate, phosphate, and salicylate adsorption indicated heterogeneity of adsorption sites on goethite (Machesky et al., 1989). Machesky and Jacobs (1991a, 1991b) suggested that adsorption enthalpies using titration calorimetry of alumina suspensions were consistent with the heterogeneity of surface functional groups proposed by the MUSIC model (Hiemstra et al., 1989a, 1989b).

Obtaining Parameter Values in Thermodynamic Surface Speciation Models

Surface Site Density

The total number of reactive surface functional groups, S_T (mol L^{-1}), an important parameter in the surface speciation models, is related to the surface site density, N_s (sites nm^{-2}):

$$S_T = \frac{Sa10^{18}}{N_A} N_S \quad [48]$$

where S is the surface area (m^2 g^{-1}), a is the particle concentration (g L^{-1}), and N_A is Avogadro's number. Experimental methods that have been used to obtain the surface site density include tritium exchange, potentiometric titration, fluoride adsorption, and maximum adsorption. Values for this parameter have also been calculated from crystal dimensions or optimized to fit experimental adsorption data. Values obtained from various determinations of surface site density vary by an order of magnitude, with tritium exchange measurements yielding the highest values. Uncertainty in surface site density is a major limitation in the standardization of SCMs, since the ability of the models to describe adsorption is sensitively dependent on this value (Goldberg, 1991). Lützenkirchen et al. (2002) showed that there are serious flaws in the use of potentiometric titrations as a means of quantifying the site density of minerals.

To allow standardization of surface complexation modeling, a fixed site density value for all minerals of 2.31 sites nm^{-2} was recommended by Davis and Kent (1990) and of 10 sites nm^{-2} by Hayes et al. (1991). Both values have been used in modeling of many natural materials. More recently, Sverjensky (2003) proposed new and more useful standard states for surface reactions, such that the equilibrium constants are independent of surface area, site density, and the amount of mineral phase present in experiments.

Applications of the DLM to metal adsorption have split the total number of reactive surface functional groups into sets of "strong" (S_s) and "weak" (S_w) adsorption sites (Dzombak and Morel, 1990). This approach almost doubles the number of adjustable parameters, since each set of sites (S_i) has its own protonation, dissociation, and metal surface complexation constants.

Koretsky et al. (1998) developed a method for estimating site types and ionizable site densities at mineral surfaces by considering ideal crystal surfaces. Surface site densities were determined using several different methods, and the results were compared to available experimental estimates of surface hydroxyl site densities. Calculated site densities based on the number of broken bonds gave the best agreement with site densities determined using the tritium exchange method. Estimates based on the number of coordinatively unsaturated atoms or on the partial charge of coordinatively unsaturated atoms were also consistent with much of the tritium exchange data. For the mineral surfaces examined by Koretsky et al. (1998), site densities on individual crystal planes ranged from 0 to 40.8 sites nm^{-2}.

Capacitances

Some values of capacitance (C in the CCM and C_1 in the TLM) can be obtained graphically from slopes of protonation–dissociation constants versus surface charge (Stumm et al., 1980). Alternatively, both capacitances, C_1 and C_2, in the TLM can be determined using an electrokinetic extrapolation technique (Sprycha, 1989a, 1989b). Experimentally determined capacitance values usually exhibit great variability; therefore, capacitances have generally been optimized to fit potentiometric titration data in simple electrolyte solutions.

Surface Complexation Constants

Values of the protonation–dissociation constants in the CCM and the TLM can be obtained experimentally from the same graphs used to obtain capacitance values. These constants can also be obtained by optimizing titration data.

Values of the surface complexation constants for ion adsorption can be obtained by fitting adsorption edges (amount adsorbed as a function of pH) or adsorption isotherms (amount adsorbed as a function of solution concentration at a single pH). These optimizations may be done with a computer program such as FITEQL (Herbelin and Westall, 1999). An advantage of computer optimization is that it yields bias-free parameters with

standard deviations and quality-of-fit criteria. Individual optimized equilibrium constant values can be weighted to obtain overall best estimates:

$$\overline{\log K} = \sum \frac{\left(1/\sigma_{\log K}\right)_i}{\sum (1/\sigma_{\log K})_i} [\log K]_i \quad [49]$$

For the DLM, a set of best estimates of log *K* values are available for a variety of adsorbing cations and anions on amorphous iron oxide (Dzombak and Morel, 1990). The advantage of this dataset is that all surface constants are self-consistent; that is, all ion surface complexation constants were optimized using the same values of protonation–dissociation constants, surface site density, and aqueous thermodynamic data. This is important because parameter values in the SCMs are interdependent (Hayes et al., 1991). Additionally, since each SCM contains a different set of assumptions for the solid–solution interface, surface complexation constants from one model cannot be used directly in any other model.

One advocated approach to addressing the problem of nonunique fits to experimental data is the adoption of a "standard" set of parameters that is uniformly applied in all systems (Davis and Kent, 1990; Dzombak and Morel, 1990; Hayes et al., 1991). While this approach may not truly represent the exact physical, electrostatic, and chemical processes operating at the mineral–water interface, it does limit the number of adjustable parameters and serves to establish a baseline that will allow future direct comparison of modeling results and the evaluation of model performance. In addition, such an approach may be desirable from the point of view of developing simple, flexible adsorption models containing internally consistent databases for performance assessment.

For example, Hayes et al. (1991) performed a sensitivity analysis of potentiometric titration data to obtain surface acidity constants for rutile, goethite, and γ-Al_2O_3. The authors considered the DLM, CCM, and TLM and investigated the effect of varying different parameters on the goodness-of-fit. Based on the results of these analyses, Hayes et al. (1991) recommended a set of "standard" parameters for each mineral and model considered.

Smith and Jenne (1991) conducted a critical evaluation of parameters for the TLM for metal cation adsorption onto iron and manganese oxides. A relationship was presented that correlated the surface complexation constant of a particular metal with its intrinsic surface complexation constant, the intrinsic acidity constant, and the cation hydrolysis constant. This relationship was found to be useful for reducing uncertainty among different investigators and for predicting unmeasured surface complexation constants for metals for which reliable hydrolysis constants are available.

In perhaps the most extensive study of available data, Dzombak and Morel (1990) performed a critical compilation of data available for adsorption of a number of cations and anions onto hydrous ferric oxide for the DLM. A number of model parameters such as mineral specific surface area and site density were fixed, and the data were optimized to obtain binding constants for 12 metal cations and 12 anions. The parameter set of Dzombak and Morel (1990) forms the basis for default values in geochemistry codes such as MINTEQA2 (Allison et al., 1990; USEPA, 1999a, 1999b; Allison Geoscience Consultants and Hydrogeologic, 2003) and PHREEQC (Parkhurst and Appelo, 1999). A similar type of database was also prepared for adsorption on goethite (Mathur, 1995).

Based on available potentiometric titration data and numerical optimization procedures, Turner (1993, 1995) developed DLM, CCM, and TLM input parameters for the acid–base behavior of a number of oxide minerals. These input parameters were used to interpret pH-dependent adsorption data for americium, neptunium, plutonium, thorium, uranium, and carbon. A uniform approach similar to that of Dzombak and Morel (1990) was used to fix a number of model parameters a priori, to limit the number of adjustable parameters, and to minimize the amount of "tweaking" necessary to improve curve fits.

A different approach has been used to establish an internally consistent set of log *K* values for the TLM for adsorption onto solid oxides and silicates (Sverjensky, 1993, 1994, 2003; Sverjensky and Sahai, 1996). Sverjensky and Sahai (1996) established equilibrium constants for surface protonation of oxides and silicates from theoretical considerations for the two-p*K* models, including minerals for which titration data were not readily available. The approach takes into account Born solvation theory for the adsorbing proton, electrostatic interactions of the adsorbing proton with a surface oxygen and an underlying metal, and an intrinsic binding of the proton to the surface. Building on the TLM dataset of surface protonation constants, Sahai and Sverjensky (1997a, 1997b) systematically established log *K* values for the adsorption of the electrolyte anion and cation and values for the capacitance C_1 from surface titration data. They found a correlation between the dielectric constant of the oxides and the log *K* values for the electrolyte cations and anions. Site densities for each oxide were determined from crystallographic considerations by Koretsky et al. (1998).

Using this pre-established database of TLM parameters for each oxide–electrolyte system (i.e., surface site densities; capacitances; and, equilibrium constants for protonation, deprotonation, electrolyte cation adsorption and electrolyte anion adsorption), Criscenti and Sverjensky (1999, 2002) used the TLM to examine experimental datasets for transition and heavy metal adsorption onto simple oxides or hydroxides. Datasets that covered a range of ionic strengths and/or surface coverages were investigated to establish stoichiometries and log *K* values for predominant metal surface complexes within the TLM framework.

Sverjensky (2001) linked the TLM capacitance values determined from data fits to the radius of the electrolyte cation. On rutile, anatase, and magnetite, the values of C_1 increased with decreasing crystallographic radius of the electrolyte cation, whereas on quartz, amorphous silica, goethite, hematite, and alumina, the values of C_1 increased with decreasing hydrated electrolyte cation radius. These results suggest that the electrolyte cations adsorbed as inner-sphere complexes to rutile, anatase, and magnetite and as outer-sphere complexes to the other oxides. This interpretation predicted distances for the adsorption of rubidium and strontium on rutile surfaces that were consistent with those measured spectroscopically by Fenter et al. (2000). Recent studies have also used Gibbs free energy minimization as an alternative to the use of equilibrium constants to describe surface reactions (Felmy and Rustad, 1998; Kulik, 2000, 2002).

More recently, Richter et al. (2003) and Brendler et al. (2003, 2004) established an adsorption database (RES^{3}T) comprising data records from many different studies for a range of minerals, including iron oxides, quartz, aluminum (hydr)oxides, titanium oxides, manganese oxides, mica, feldspars, and clay minerals. The database contains mineral properties, specific surface area values, characteristics of surface binding sites and their protolysis, and surface complexation reactions. An extensive bibliography is included, providing links to the experimental data and background information concerning details of SCM parameter selection, surface species evidence, and adsorption experiment techniques. The RES^{3}T database contains more than 1400 literature references.

The Common Thermodynamic Database Project, CTDP (van der Lee and Lomenech, 2004) is another database that includes adsorption equilibrium constants for SCMs. At present, the CTDP database includes 330 surface species for nine solids.

The values of SCM parameters are imperfectly known, and in practice they have tended to be used as multiple fitting parameters specific to a particular dataset. Given the number of parameters involved, this almost certainly led to nonunique fits to experimental data. Also, because of fundamental differences in how the models treat the mineral–water interface and the tendency to use model-specific nonstandard parameters, it is often difficult to compare directly the results of different studies and even more difficult to compare the performance of different models for a given dataset.

Applications

Applying Surface Complexation Models to Single Mineral Phases

The CCM has been applied to describe adsorption on aluminum, iron, silicon, and titanium oxides, kaolinite, illite, and montmorillonite clay minerals, plant cell walls, and soils. Adsorbing ions that have been studied include the cation and metal ions: aluminum, cadmium, calcium, cesium, cobalt, copper, iron, lead, manganese, mercury, nickel, silver, zinc, europium, lanthanum, and ytterbium; and the anions: arsenate, arsenite, borate, fluoride, molybdate, phosphate, selenite, silicate, selenate, sulfate, benzoate, citrate, phthalate, and salicylate.

The DLM has been applied to describe adsorption on aluminum, iron, manganese, silicon, and titanium oxides, biotite, kaolinite, and montmorillonite clay minerals, natural organic matter, bacterial cell walls, and sediments. Adsorbing ions that have been studied include the cation and metal ions: aluminum, barium, cadmium, calcium, chromium, cobalt, copper, lead, mercury, nickel, silver, strontium, zinc, and uranium; and the anions: arsenate, arsenite, borate, chromate, fluoride, phosphate, sulfate, selenite, selenate, vanadate, benzoate, oxalate, phthalate, salicylate, thiosulfate, and fulvate. Adsorption of various metal ions has been studied on a lignocellulose organic substrate extracted from wheat bran (Ravat et al., 2000). These applications considered two sets of reactive surface functional groups representing carboxylic and phenolic sites. The DLM was able to describe copper adsorption on this natural material.

The TLM has been applied to describe adsorption on aluminum, iron, manganese, and silicon oxides, kaolinite and smectite clay minerals, and soils. Adsorbing ions that have been studied include the cation and metal ions: cadmium, calcium, cobalt, copper, lead, magnesium, mercury, potassium, silver, sodium, zinc, neptunium, plutonium, thorium, and uranium; and the anions: arsenate, arsenite, borate, chloride, chromate, fluoride, molybdate, nitrate, perchlorate, selenite, selenate, silicate, sulfate, acetate, carbonate, formate, lactate, oxalate, phthalate, salicylate, and humate.

The one-pK model has been applied to describe adsorption on aluminum, iron, and titanium oxides. Most studies to date have used goethite as the adsorbent material. Adsorbing ions that have been studied include the cations: cadmium, calcium, copper, and potassium; and the anions: arsenate, chromate, phosphate, selenite, sulfate, citrate, lactate, malonate, oxalate, phthalate, and fulvate.

Applying Surface Complexation Models to Natural Mineral Assemblages

An important advantage of the SCM approach applied to natural materials is the linkage between aqueous speciation modeling and the calculation of adsorption via the coupling of mass law equations. In addition, the SCM approach allows a simple description of the dependence of adsorption on pH (Davis et al., 1998) that is conceptually more appealing and more useful for predictive modeling than the empirical statistical K_d approach.

For natural materials uncertainties exist in applying SCMs because of the physical and chemical heterogeneity of natural soils and sediments. Two approaches have been applied to describe adsorption on heterogeneous materials: the CA approach (Honeyman, 1984) and the GC approach. The CA approach is based on summing the adsorption by the individual component minerals of a soil or sediment to obtain a measure of the total adsorption of the mixture. The summation can occur as the sum of results for thermodynamic surface speciation models or as the sum of pseudo-thermodynamic models for adsorption on individual mineral phases. Pseudo-thermodynamic models include models without electrostatic correction terms, sometimes called nonelectrostatic models (NEMs). Because the modeling approach is based on summing the results from models already calibrated with pure mineral phases, the CA approach is predictive and does not involve fitting adsorption data for the natural materials.

Extending the models to natural samples necessitates certain approximations and modifications. For example, in the application to clay minerals or soils, the assumption is usually made that adsorption occurs through interaction with the hydroxyl groups at the edges of clay particles. The effect of permanent negatively charged sites at the clay basal planes on adsorption is usually ignored. This simplification may not be appropriate, especially for anions, whose edge site adsorption may be affected by the permanent negative charge. An additional assumption is that the constituent minerals are uncoated and do not interact. This assumption is violated in sediments and soils.

In the GC modeling approach, the surface of the mineral assemblage is considered too complex to be quantified in terms of the contributions of individual phases to adsorption. Instead, it is assumed that adsorption can be described by SCM equilibria written for "generic" surface functional groups, with the stoichiometry and formation constants for each SCM mass law evaluated on the basis of simplicity and goodness-of-fit (Davis

et al., 1998, 2002, 2004a). The generic surface sites represent average properties of the soil or sediment surface rather than specific minerals. Experimental data for site-specific natural materials must be collected over the field-relevant range of chemical conditions. The model parameters are likely not transferable to other field sites. This GC modeling approach results in models calibrated with conditional parameters that are valid only for the range of aqueous chemical conditions considered in the experimental dataset. For predictive purposes, interpolation of chemical conditions within the ranges tested in the experiments is valid, but extrapolation to values outside these ranges is not (Davis et al., 2005). Therefore, a larger experimental dataset improves the robustness of the model and its usefulness for predictive calculations. A NEM can be used in a GC approach because the pH-dependent coulombic factor will be included indirectly in the fitting via log *K* values, reaction stoichiometries, or site densities.

Applications of the CCM to soils have been limited to the description of anion adsorption. The model has been used to describe phosphate (Goldberg and Sposito, 1984), borate (Goldberg, 1999, 2004; Goldberg et al., 2000, 2004, 2005a), selenite (Goldberg and Glaubig, 1988b; Sposito et al., 1988), arsenate (Goldberg and Glaubig, 1988a, Goldberg et al., 2005b), sulfate (Kooner et al., 1995), and molybdate (Goldberg et al., 1998, 2002) adsorption on soils using a GC approach. In these studies the electrostatic terms and protonation–dissociation constants were retained. Except in the study of Kooner et al. (1995), values of the protonation and dissociation constants were averages obtained from a literature compilation of values for aluminum and iron oxide minerals. Kooner et al. (1995) obtained protonation and dissociation constant values by optimizing potentiometric titration data. Monodentate anion surface species were defined in all studies. In addition to monodentate selenite species adsorbed on one set of surface sites, Sposito et al. (1988) assumed that bidentate selenite species formed on another set of surface sites. To describe borate (Goldberg, 1999) and selenite (Goldberg and Glaubig, 1988b) adsorption, values of the protonation and dissociation constants were optimized together with the anion surface complexation constants.

The predictive ability of the CCM to describe ion adsorption has been tested for phosphate (Goldberg and Sposito, 1984), borate (Goldberg and Glaubig, 1986, Goldberg et al., 2000, 2004, 2005a), selenite (Sposito et al., 1988), molybdate (Goldberg et al., 2002), and arsenate (Goldberg et al., 2005b). Qualitative prediction of selenite adsorption on four California soils was possible using the selenite surface complexation constants obtained for one other California soil (Sposito et al., 1988). The model was qualitatively able to predict phosphate (Goldberg and Sposito, 1984) and borate (Goldberg and Glaubig, 1986) adsorption on individual soils using an average set of anion surface complexation constants obtained from numerous soils.

A new approach for predicting boron adsorption used a general regression model to predict CCM surface complexation constants from the easily measured soil physical and chemical properties: surface area, organic and inorganic carbon content, and aluminum oxide content (Goldberg et al., 2000, 2004, 2005a). This approach was well able to predict boron adsorption by numerous soils of diverse soil orders having a wide range of chemical properties and provided a completely independent model evaluation. The prediction equations developed from describing boron adsorption on a set of soils primarily from California were able to predict boron adsorption on a set of soils from the midwestern USA, suggesting wide applicability of the prediction approach (Goldberg et al., 2004). The original prediction equations developed for boron adsorption as a function of solution pH at a concentration of 5 mg B L^{-1} on southwestern soils were able to describe boron adsorption as a function of solution boron concentration up to 250 mg B L^{-1} on midwestern soils. A similar modeling approach was used to predict molybdate adsorption on a wide range of soils (Goldberg et al., 2002). The general regression equations predict CCM molybdenum surface complexation constants from the chemical properties: cation exchange capacity, organic and inorganic carbon content, and iron oxide content. This approach was also used to predict arsenate adsorption on a large set of soils using five soil chemical properties to predict the arsenate surface complexation constants in the CCM (Goldberg et al., 2005b).

Davis and Curtis (2003) studied the Uranium Mill Tailings Remediation Action (UMTRA) site near Naturita, CO, because it had a well-developed and definable uranium(VI) plume in a shallow alluvial aquifer and had spatially variant chemical conditions, expected to influence transport and retardation. Laboratory batch and column experiments showed that the adsorption and retardation of uranium(VI) by the Naturita sediments was strongly influenced by the dissolved carbonate concentration. A GC model was developed for the Naturita aquifer background sediments based on fitting batch uranium(VI) adsorption data. Using only two surface reactions (four surface species), the GC NEM model was able to accurately simulate K_d values for uranium(VI) adsorption on the Naturita aquifer sediments over the observed range of pH and dissolved carbonate and uranium(VI) concentrations.

The CA and GC modeling approaches were compared for U(VI) adsorption by sediments from the Koongarra natural analog site located in northwest Australia (Waite et al., 2000; Davis et al., 2002). The CA approach necessitated eight reactions and used a diffuse double layer electrostatic model, whereas the GC approach required only four surface reactions and did not include an electrostatic model. The performance of the two modeling approaches was nearly identical, even though the GC model contained 7 model parameters and the CA model contained 11. A similar intercomparison of CA and GC diffuse layer modeling approaches on the same data was performed by 12 teams from eight countries (Payne et al., 2004). CA simulations were unable to provide satisfactory descriptions of the data, and reoptimization of some parameter values was necessary. Generalized composite models provided better simulations of the data but optimized a greater number of parameters. The ability of either approach to describe uranium(VI) adsorption on other rock samples from the same field site was unsatisfactory.

Difficulties in Applying Thermodynamic Surface Speciation Models to Natural Systems

The thermodynamic surface speciation and semi-empirical modeling approaches represent two extremes of surface complexation modeling (see Table 2 and Davis et al., 1998, 2004a). In thermodynamic surface speciation models (e.g., Hiemstra and van Riemsdijk, 1999), the surface species postulated should be

TABLE 2. Characteristics of surface complexation modeling approaches for environmental adsorbents.

Thermodynamic surface speciation modeling†	Semi-empirical modeling
Adsorption is predicted from thermodynamic constants and known (confirmed) surface species	Adsorption data are simulated (fit) using site-specific adsorbent samples, using chemically plausible surface reactions
Surface sites are unique and defined for each specific mineral phase present in environmental samples	Generic surface sites are assumed, with average chemical characteristics
Surface site densities are quantified by detailed characterization of the surface of environmental samples	Surface site densities are quantified by the measurement of specific surface area or by fitting adsorption data of environmental samples
Apparent stability constants and reaction stoichiometries are obtained from studies of adsorption by reference mineral phases present in environmental samples	Apparent stability constants and reaction stoichiometries are fit to experimental adsorption data for environmental samples or model constants are predicted based on regression to soil properties and fitted constants
Overall adsorption is predicted by the sum of adsorption calculated for each specific mineral phase present in environmental samples	Numbers of surface site types and chemical reactions are increased as necessary to achieve good model simulations and to meet modeling objectives

† Thermodynamic surface speciation models that are developed by predicting adsorption as the sum of contributions from individual mineral phases are called component additivity (CA) models (Davis et al., 2002, 1998; Honeyman, 1984). Characteristics for thermodynamic surface speciation modeling in Table 2 apply to the CA modeling approach.

supported with spectroscopic evidence. Thermodynamic surface speciation models usually include electrical double layer terms in the mass law equations, and hence, adsorption predictions with these models are sensitive to the double layer parameters.

The sensitivity to electrostatic terms illustrates a significant practical problem in extending thermodynamic surface speciation models directly to simulate metal ion adsorption on complex mineral assemblages in the environment. Mineral surfaces in the environment are typically coated with poorly crystalline secondary mineral coatings, as has been shown in detail for many different sediment samples (e.g., Coston et al., 1995). The coatings make it extremely difficult to quantitatively assess the electrostatic contribution to the free energy of adsorption. In the literature, one frequently finds the assumption that the electrical double layer properties of pure mineral phases studied in the laboratory are the same as in a mineral assemblage found in the environment (e.g., Arnold et al., 2001). Current understanding of bonding is well advanced at the molecular scale (e.g., Bargar et al., 2000; Arai et al., 2006), but our understanding and models become increasingly uncertain as the physical scale increases. The adsorption of ions by sediments and soils is ultimately controlled by adsorptive phases with dimensions on the order of tens of nanometers.

It seems unlikely that modeling assumptions based on pure mineral phases are valid, given the reality of small-scale heterogeneities and coatings prevalent in soils and sediments. In addition, the CA modeling approach is difficult to apply because the site densities of the mineral and organic phases in the coatings that are contributing to metal ion adsorption are unknown (Davis et al., 2002). This inherent heterogeneity of environmental samples makes application of the thermodynamic surface speciation models difficult at present, even at the microscale level.

While a thermodynamic surface speciation model must be validated with spectroscopic evidence and other detailed data to confirm surface speciation and electrical double layer properties (Hiemstra and van Riemsdijk, 1999), the GC modeling approach is more easily applied, and fewer experimental data need to be collected. The range of applicability of a GC model with respect to chemical variation is determined by the type and amount of experimental data collected. Generalized composite model parameters are calibrated by fitting a simple surface speciation model so that the major features of adsorption are simulated as chemical conditions are varied over field-relevant ranges (Davis et al., 1998).

Subsurface Transport Modeling

The retardation of inorganic contaminants during groundwater transport can be influenced strongly by the variability in chemical conditions over the spatial or temporal domain of the model (Reardon, 1981; Bethke and Brady, 2000). For traditional modeling that relies on adsorption isotherms, various approaches have been proposed to describe the influence of variable chemistry on isotherm parameters. For example, in describing the influence of variable groundwater on lithium retardation, Brusseau and Srivastava (1999) used different K_d values in different hydrogeochemical regimes. Other authors (van der Zee and van Riemsdijk, 1987; USEPA, 1999b) have made isotherm parameters explicit functions of key aqueous chemical variables. Boekhold and van der Zee (1992) and Streck and Ritcher (1997) used this approach to describe the influence of pH on the field-scale variability of adsorptive properties of soils. Water–mineral interactions during transport can influence aqueous chemical composition and result in a significant indirect effect on the transport of adsorbing solutes (Kohler et al., 1996; Scheidegger et al., 1994; Meeussen et al., 1996).

Subsurface Transport Modeling Using the Surface Complexation Concept

Transport models that include SCMs to describe adsorption have been used in only a few field-scale applications. Stollenwerk (1995) calibrated a DLM to simulate molybdate transport in laboratory columns and then successfully predicted molybdenum transport in a shallow sand and gravel aquifer on Cape Cod (Stollenwerk, 1998).

Kent et al. (2000) successfully simulated the pH-dependent transport of zinc in the Cape Cod aquifer with a GC model for zinc adsorption. Generalized composite model adsorption parameters were determined in independent laboratory experiments. A 59-yr simulation with a one-site adsorption model was well able to describe the influence of pH on zinc transport. Simulation with a two-site adsorption model described both the sharpness and approximate location of the leading edge of the zinc contaminated region. The influence of variable pH on the adsorption and transport of zinc was accomplished much more easily with the semi-empirical GC DLM than could be achieved with distribution coefficients or adsorption isotherms. The transport predictions were made without adjusting any adsorption model parameters.

Curtis et al. (2006) used two-dimensional reactive transport modeling to simulate uranium(VI) transport in an alluvial

aquifer at a former uranium ore processing mill near Naturita, CO. The model was based on an independently calibrated flow model and the independently calibrated GC model for uranium(VI) adsorption. K_d values were calculated from the simulated concentrations. Transport simulations conducted for the field scale demonstrated the importance of using the GC model to describe uranium(VI) adsorption rather than a constant K_d modeling approach (Curtis et al., 2006). A major conclusion from the transport simulations was that risk assessment modelers must recognize not only that variable chemical conditions can cause a range of K_d values to be observed but also that the spatial distribution of K_d values within that range is not likely to be a random function or a normal distribution. The simulations also showed that predicted uranium(VI) transport was nearly identical whether or not surface charge was explicitly considered within the adsorption model. Davis and Curtis (2003) conducted transport experiments in columns packed with Naturita sediments to investigate the effects of variable chemical conditions on uranium(VI) transport. The results showed that uranium(VI) retardation was significantly affected by variable chemical conditions, especially variable alkalinity and pH. The observed variations in uranium(VI) retardation were predicted reasonably well by the same transport model used in field simulations that included the GC adsorption model and assumed local chemical equilibrium.

Vaughan et al. (2004) used the UNSATCHEM model (Suarez and Simunek, 1997) to predict boron transport within an agricultural field irrigated with boron containing water. The CCM surface complexation constants were estimated by using a set of regression relationships based on soil properties (Goldberg et al., 2000). The model was only partially successful in predicting the spatial distribution of boron concentrations in the soil, likely due to lack of information on the spatial variability of water infiltration.

Spatial Heterogeneity of Aquifer Sediment Properties

The effect of aquifer heterogeneity on reactive solute transport has been the focus of several studies in contaminant hydrology (Bosma et al., 1993; Burr et al., 1994). The depositional processes forming sedimentary aquifers produce heterogeneities such as interbedding, discontinuous lenses, or strata of differing grain-size and mineralogical composition. These heterogeneities create zones of variable permeability in aquifers, which may increase the dispersion of solutes relative to that expected in a homogeneous aquifer (Gelhar and Axness, 1983; Garabedian et al., 1991; Hess et al., 1992). As discussed previously, the spatial heterogeneities of grain-size and primary and secondary mineral abundance also result in variability in reactive and absorbent phases (Barber, 1994; Friedly et al., 1995). In addition, the distribution and reactivity of mineral phases within a sedimentary aquifer can vary with the degree of pre- and postdepositional weathering of the sediments. Heterogeneity in mineral phase abundance may enhance the spreading of reactive solutes during transport, for example, when there is a negative correlation between hydraulic conductivity and the partition coefficient for an adsorbing ion (Bosma et al., 1993; Burr et al., 1994). Knowledge of the spatial variability of adsorption properties within an aquifer and their degree of correlation with hydraulic conductivity may be critical for improving predictive transport modeling efforts (Robin et al., 1991; Bosma et al., 1993; Burr et al., 1994). However, characterization of field-scale variability of adsorption properties within an aquifer poses a significant challenge.

Fuller et al. (1996) quantified the variability of lead and zinc adsorption onto sediments from the Cape Cod aquifer at a spatial scale of tens of meters. The variability in lead and zinc adsorption was significantly correlated with extractable iron and aluminum from sediment coatings. The variability in adsorption was best described by the variability in iron and aluminum oxide coating abundance when the results were normalized to a constant surface area basis. Lead and zinc adsorption on the sediments only varied by a factor of three for 38 samples collected within a spatial domain of 0.5 km in the direction of groundwater flow. This result suggests that using the "average" properties of aquifer sediments may be adequate for field-scale adsorption modeling at the kilometer scale. At larger scales, average properties of sediments may need to be determined for each geological unit.

Goldberg et al. (2005a) evaluated the predictive ability of the CCM to describe boron adsorption as related to changes in clay content on a field scale. The model was able to predict boron adsorption at five soil depths at three sites using the surface complexation constants predicted with the chemical properties of one of the surface depths and a surface area value calculated from clay content. Thus, these soil chemical properties can be measured at various locations throughout a field without significantly altering the quality of the predictions of boron adsorption. This finding significantly reduces the need for tedious, costly, and time-consuming boron adsorption experiments. Additional corroborative work is needed at other field sites to evaluate whether this approach can be generalized beyond the field scale to the basin scale.

Field Methods for Testing Adsorption Models and Model Parameters

Davis and Curtis (2003) investigated methods to estimate uranium(VI) K_d values at the Naturita field site using data from uncontaminated sediments. Such methods are needed (i) for validation of SCM parameters for transport simulations within risk assessment models and (ii) for estimation of initial conditions for adsorbed contaminants for transport simulations describing previously contaminated sites. Uranium(VI) K_d values predicted with a GC adsorption model generally agreed to within a factor of two to three with experimental estimates of the K_d values for uranium contaminated sediments (Kohler et al., 2004). This agreement with the experimental determinations of adsorbed uranium(VI) in the contaminated portion of the Naturita alluvial aquifer provides confidence in the predictive capability of a GC adsorption model within field-relevant conditions.

Choice of Conceptual Model for Adsorption in Subsurface Transport Modeling

The different federal agencies, U.S. Department of Defense, USDOE, NRC, USEPA, ARS, and USGS, use a number of different computer codes to simulate reactive contaminant transport. The basic conceptual models available in different codes are summarized in Table 3. Information on sources for model parameters in the different codes is summarized in Table 4. Most

TABLE 3. Conceptual adsorption models used by Memorandum of Understanding agency reactive transport codes.

Codes†	Empirical adsorption		Kinetic adsorption	Thermodynamic adsorption‡	
	Linear§	Nonlinear		Electrostatic (surface complexation model type)	Nonelectrostatic
2D- and 3D-FATMIC (USEPA)	K_d (R_f)				
ARAMS (DoD, Army Corps of Engineers)	K_d (R_f)				
BIOMOC (USGS) (see MOC3D)	K_d (R_f)				
CHEMFLO (USEPA)	K_d (R_f)				
CRUNCH (USDOE)				DLM	
DandD (USEPA)	K_d (R_f)				
EPACMTP (USEPA)	K_d	Freundlich			
GMS-ART3D (USDoD, Army Corps of Engineers)	R_f				
GMS-FEMWATER (USDoD, Army Corps of Engineers)	K_d	Langmuir, Freundlich			
GMS-MODFLOW (USDoD, Army Corps of Engineers) (see MOC3D)	K_d				
GMS- MT3DMS (USDoD, Army Corps of Engineers)	K_d	Freundlich, Langmuir	Nonequilibrium: kinetic first order, irreversible		
GMS-NUFT (USDoD, Army Corps of Engineers)	K_d				
GMS- RT3D (USDoD, Army Corps of Engineers)	K_d	Freundlich, Langmuir	Rate limited adsorption simulated using first-order mass transfer rate to calculate effective Rf		
GMS-SEAM3D (USDoD, Army Corps of Engineers)	K_d				
GMS-UTCHEM (USDoD, Army Corps of Engineers) (see also UTCHEM)	K_d (organics, tracers, gel retention)	Langmuir (polymers, organics, Cr, and surfactants) Freundlich (organics)			Includes ion exchange for major ions and Cr, Pb
HST3D (USGS)	K_d				
HYDRUS-1D, HYDRUS-2D (USDA)	K_d	Nonlinear cation adsorption	Nonequilibrium cation adsorption		
MEPAS (USDOE)	K_d				
MOC3D (USGS) (see also BIOMOC, MODFLOW)	K_d (R_f)				
MODFLOW (USGS) (see also MOC3D)	K_d (R_f)				
MULTIMED (USEPA)	K_d (R_f)				
PHREEQC (USGS)		Langmuir, Freundlich		DLM	Included, not specified
PRESTO (USEPA)	K_d (R_f)				
RATEQ (USGS)					Ion exchange and SCM
RESRAD (USDOE)	K_d				
R-UNSAT (USGS)	K_d				
SWAT (USDA)	K_d (pesticide only)				
TPA (NRC)	K_d				
TSPA-SR (USDOE)	K_d				
UNSATCHEM (USDA)	K_d			CCM	Includes ion exchange for major cations
UTCHEM (USEPA) (see also GMS-UTCHEM)	K_d (organics, tracers, gel retention)	Langmuir (polymers, organics, Cr, and surfactants) Freundlich (organics)			Includes ion exchange for major ions Cr, Pb
VLEACH (USEPA)	K_d (VOC and semivolatile organics)				

† NRC, U.S. Nuclear Regulatory Commission; USDoD, U.S. Department of Defense.
‡ CCM, constant capacitance model; DLM, diffuse layer model; SCM, surface complexation model.
§ K_d, linear distribution coefficient; R_f, retardation coefficient; VOC, volatile organic compound.

of these codes rely on adsorption isotherms (K_d, Freundlich, and Langmuir) and provide a set of default input values. In some cases, input is user-specified. These tables are not intended to be an exhaustive list or to provide detailed information about the implementation of adsorption models in the different codes. The readers are referred to the code documentation for more detail.

It is recognized that fully empirical models are simpler in mathematical construction, and because of the relatively straightforward application of these models, abundant experimental data have been generated to determine the necessary empirical coefficients for a variety of elements and substrates. However, this simplicity comes at the expense of flexibility. The fully empirical nature of these models tends to lump processes together and cannot adequately discriminate between the effects of various physical–chemical parameters that may compete and interact in a complex manner to control contaminant retardation. Since empirical models do not provide mechanistic understanding of adsorption processes, extrapolation beyond the experimental conditions used to generate the data fitted by the model is unjustified.

As the theoretical basis for the conceptual models for adsorption increases, the flexibility and applicability of the model generally increases as well. Thermodynamic surface speciation models

TABLE 4. Input parameter sources for Memorandum of Understanding agency reactive transport codes.

Code†	Parameter source	Website(s)	Comment‡
2D- and 3D-FATMIC (USEPA)	User-specified input	http://www.epa.gov/ada/csmos/models/2dfatmic.html; http://www.epa.gov/ada/csmos/models/3dfatmic.html	Designed for organic transport and bioremediation evaluation. Fate and transport through saturated-unsaturated media of seven components (one substrate, two electron acceptors, one trace element, and three microbial populations) are modeled. Includes subroutines for microbe-chemical interaction.
ARAMS (USDoD, Army Corps of Engineers)	User-specified input; database (FRAMES)	http://www.wes.army.mil/el/arams/arams.html	Input parameters through MEPAS; to be combined with GMS suite of codes.
BIOMOC (USGS) (see MOC3D)	User-specified input	ftp://water.usgs.gov/pub/software/ground_water/biomoc/doc/biomoc.pdf	Based on MOC3D. Organic compound transport only, includes biodegradation by first-order decay.
CHEMFLO (USEPA)	User-specified input	http://www.epa.gov/ahaazvuc/csmos/models/chemflo.html	1D transport with homogeneous aquifer properties. Includes graphic and tabular output options. Batch input, with preprocessing by sequence of DOS menus. Chemical degradation simulated with first-order decay.
CRUNCH (USDOE)	User-specified input	http://www.csteefel.com; http://www.pnl.gov.cse/subsurface/crunch.htm	Coupled reaction and transport processes. Includes ion exchange, precipitation/dissolution. Thermodynamic data from EQ3/6 database. Precipitation and dissolution of adsorbent phase allowed.
DandD (USDOE)	Default values can be overridden by user-specified input.	http://techconf.llnl.gov/radcri/java.html	Default values from compilation of Sheppard and Thibault (1990). Value of K_d = 0 assigned to mobile species.
EPACMTP (USEPA)	User-specified input; internally computed through organic carbon fraction, auxiliary database based on groundwater pH	http://www.epa.gov/epaoswer/non-hw/industd/tools/cmtp/tbd_toc3.pdf	pH-dependent K_d values can be calculated off-line using geochemical programs such as PHREEQC or MINTEQA2. Also includes organic adsorption with linear isotherm (K_{oc}).
GMS-ART3D (USDoD, Army Corps of Engineers)	User-specified input	http://gms.watermodeling.org/ftp/products/gms/docs/tutor40%20vol4.pdf	GMS is a high-order executive that provides common pre- and postprocessing GUI options for groundwater modeling codes developed by different Federal agencies.
GMS-FEMWATER (USDoD, Army Corps of Engineers)	User-specified input	http://gms.watermodeling.org/ftp/products/gms/docs/Femwater.pdf	
GMS-MODFLOW (USDoD, Army Corps of Engineers) (see also MODFLOW, MOC3D)	User-specified input	ftp://water.usgs.gov/pub/software/ground_water/modflow/doc/ofr00-92.pdf	
GMS-MT3DMS (USDoD, Army Corps of Engineers)	User-specified input	http://hydro.geo.ua.edu/mt3d/mt3dmanual.pdf http://gms.watermodeling.org/ftp/products/gms/docs/tutor40%20vol2.pdf	
GMS-NUFT (USDoD, Army Corps of Engineers)	User-specified input	http://www.bossintl.com/ftp/products/gms/docs/nuftII_v2.pdf	
GMS-RT3D (USDoD, Army Corps of Engineers)	User-specified input	http://bioprocess.pnl.gov/publictn/PNNL_11720_RT3Dv1_Manual.pdf	
GMS-SEAM3D (USDoD, Army Corps of Engineers)	User-specified input	http://gms.watermodeling.org/html/seam3d.html	
GMS-UTCHEM (USDoD, Army Corps of Engineers) (see also UTCHEM)	User-specified input	http://www.epa.gov/ada/download/reports/napl3d.pdf http://gms.watermodeling.org/ftp/products/gms/docs/chemtech.pdf	
HST3D (USGS)	Not specified	http://wwwbrr.cr.usgs.gov/projects/GW_Solute/hst/index.shtml http://water.usgs.gov/software/hst3d.html	Simulates heat and solute transport in three-dimensional saturated ground-water porous media for a single-solute species that may decay and may adsorb onto the porous medium.
HYDRUS-1D, HYDRUS-2D (USDA)	User-specified input; Auxiliary database	http://typhoon.mines.edu/software/igwmcsoft/hydrus1d.htm http://typhoon.mines.edu/software/igwmcsoft/hydrus2d.htm	Inverse parameter estimation from transient or steady-state solute transport data
MEPAS (USDOE)		http://mepas.pnl.gov/earth/mepasform.html	Default values require a value for pH, total clay, NOM, and iron/aluminum oxides. Divided into nine different categories.
MOC3D (USGS)	User-specified input	http://water.usgs.gov/nrp/gwsoftware/moc3d/moc3d.html	MOC3D includes a number of other supporting codes for preprocessing and postprocessing, and is integrated with the MODFLOW family of codes. MOC2D allows nonlinear adsorption isotherms
MODFLOW (USGS) (see also GMS-MODFLOW, MOC3D)	User-specified input	http://water.usgs.gov/nrp/gwsoftware/modflow.html	MFI2K data input program for MODFLOW. Numerous updates and GUI pre- and postprocessors developed since first publication (1984)
MULTIMED (USEPA)	Default values can be overridden by user-specified input.	http://www.epa.gov/ceampubl/mmedia/multim2/index.htm http://www.scisoftware.com/products/multimed_overview/multimed_overview.html	Includes interactive pre- and postprocessor GUIs. Simulates transient, one-dimensional (vertical) transport in the unsaturated zone and steady-state or transient, semi-analytical saturated zone transport.
PHREEQC (USGS)	User-specified input; auxiliary database	http://wwwbrr.cr.usgs.gov/projects/GWC_coupled/	Mole fraction standard state for activity of surface species. Includes 1D transport calculations with equilibrium and nonequilibrium chemical reactions (precipitation and dissolution, ion exchange)
PRESTO (USEPA)	User-specified input	http://www.epa.gov/radiation/assessment/presto.html	Developed for radionuclide transport through soils. Includes radioactive decay, atmospheric dispersion, and dose calculations.

TABLE 4. Continued.

Code†	Parameter source	Website(s)	Comment‡
RESRAD (USDOE)	Default values can be overridden by user-specified input.	http://web.ead.anl.gov/resrad/	Default values from available literature, mostly pre-1981.
R-UNSAT (USGS)	User-specified input	http://nj.usgs.gov/toxics/models.html#R-UNSAT	Gas transport of VOC with biodegradation. Can also be used for radon migration.
SWAT (USDA)	User-specified input	http://www.brc.tamus.edu/swat/swatmod.html ftp://ftp.brc.tamus.edu/pub/swat/doc/swatuserman.pdf	Mostly for surface water and runoff transport of pesticides, but also includes transport of pesticides through soil profile to aquifer.
TPA (NRC)	Default probability distributions can be overridden by user-specified input	http://www.nrc.gov/reading-rm/adams/web-based.html	Default includes probability density functions for K_d values based on expert elicitation, laboratory data, and SCM modeling
TSPA (USDOE)	Default probability distributions can be overridden by user-specified input	http://www.ocrwm.doe.gov/documents/sl986m3b/index.htm	Default includes probability density functions for K_d values based on expert elicitation, laboratory data
UNSATCHEM (USDA)	User-specified input; solution to transport equations	ftp://ftp.ussl.ars.usda.gov/models/unsatchm/unsatchm.pdf	CO_2 production, CO_2 and solute transport, cation exchange, precipitation and dissolution for major ions and CCM for B.
UTCHEM (USEPA) (see GMS-UTCHEM)	User-specified input	http://www.epa.gov/ada/csmos/models/utchem.html	3D transport of organic compounds (NAPL) and inorganic compounds in vadose and saturated zones. Includes EQBATCH geochemistry subroutine with aqueous complexation, precipitation, dissolution, and ion exchange for major ions plus Cr and Pb. Includes organic adsorption with linear isotherm (K_{oc}). Includes biodegradation.
VLEACH (USEPA)	Default values specified in users manual, can be overridden by user-specified input.	http://www.epa.gov/ada/csmos/models/vleach.html	1D transport of organic compounds only. Includes organic adsorption with linear isotherm (K_{oc}). K_d calculated based on K_{oc} and fraction of organic carbon (f_{oc}) No biodegradation or consideration of density flow of NAPLs.

† NRC, U.S. Nuclear Regulatory Commission; USDoD, U.S. Department of Defense.
‡ CCM, constant capacitance model; GUI, graphic unit interface; K_d, linear distribution coefficient; NAPL, nonaqueous phase liquid; SCM, surface complexation model; VOC, volatile organic compound.

use theoretical relationships governing interaction between an electrolyte solution and a charged substrate of a particular structure and composition. By explicitly defining the relationships between a number of system parameters, these models are much more robust and can be extended with less uncertainty beyond experimental conditions to a wide range of environments. As sophistication increases, however, the data requirements and the number of adjustable parameters increase as well. Much of the data necessary for rigorous application of these models is frequently unavailable, poorly constrained, or only available for pure or synthetic minerals. This makes extrapolation to natural solid solutions and composite materials difficult. Uncertainty with regard to the electrostatic behavior of heterogeneous materials has led to the development of semi-empirical, nonelectrostatic SCMs. These models eliminate the electrostatic terms from the mass-action expressions and are a compromise between fully empirical adsorption models using lumped parameters and more complex representations of the mineral–water interface. They contain fewer parameters than do full electrostatic models. However, these models are limited to the geochemical conditions at a specific field site and are not generally applicable.

One of the potentially large uncertainties in risk assessment model calculations arises from the choice of K_d values for individual contaminants. Depending on the type and purpose of the modeling, either a single K_d value may be chosen from tabulated databases for each contaminant or a probability distribution function may be derived that encompasses a range of K_d values. The uncertainty in the choice of K_d values or in the probability distribution function arises from several sources, such as experimental error, extrapolation or interpolation of values to chemical conditions or rock types other than those used in actual experimental measurements of K_d, and the scaling of K_d values measured for rock powders to the values expected for intact rocks in the site-specific, geologic setting.

For a variety of reasons, the range of K_d values that may need to be considered for each contaminant–rock combination can be quite large. One can consider spatial and temporal variability in chemical conditions in risk assessment modeling using K_d values by separating the calculations into separate blocks of time or hydrologic units in space. However, it is not unusual at field sites contaminated by point sources to find other co-solutes that form plumes, in addition to the contaminants of interest. Although the effects of changes in chemical conditions on the solubilities of contaminants can usually be calculated in a straightforward manner, the effects of variable chemical conditions on adsorption and the choice of K_d values are more complex (Davis et al., 2002; USEPA, 1999b; Kohler et al., 1996). To be conservative, large ranges of K_d values may need to be estimated by expert judgment to account for possible changes in chemical conditions and for other sources of error. The uncertainties in these ranges are difficult to assess quantitatively without doing large numbers of experiments.

Surface complexation modeling could be of significant value to risk assessment calculations, even if it is only used to determine the range of K_d values that needs to be considered and to provide a scientific basis for the range of values chosen. Uncertainties in SCM parameters can be less than the uncertainties in K_d values (taking into account the robustness over a range

of chemical conditions), and SCM uncertainties may be more easily quantified. For example, a recent report on batch studies of uranium(VI) adsorption on montmorillonite presented K_d values that varied by more than four orders of magnitude over the pH range 6.5 to 8.5 (Pabalan and Turner, 1996). Davis et al. (1998) and Kent et al. (2000) showed that the K_d values for zinc in a sand and gravel aquifer varied by about two orders of magnitude because of variable chemical conditions in the groundwater. In each of these cases, the datasets could be described by an SCM with a small number of independent parameters that remained constant and had comparatively less uncertainty in their values.

Using a range of four orders of magnitude in the uncertainty of K_d values, for example, could inadvertently lead to risk dilution, increased costs for waste cleanup at an industrial site, or rejection of an effective alternative waste disposal scenario. If used properly, SCMs for contaminant adsorption have the potential to increase the confidence and scientific credibility of transport modeling by reducing the uncertainty in quantifying retardation and providing a means of quantifying that uncertainty. In addition, SCMs have the potential to lower the estimated remediation costs of sites (or to support the feasibility of a disposal scenario) by decreasing the uncertainty of K_d values (and the associated safety factor applied in risk assessment modeling). Finally, the use of SCMs can provide a stronger basis for applications of natural attenuation in contaminated systems (Brady et al., 1999).

In support of the NRC's Total System Performance Assessment (TPA) code for the geologic disposal of high-level radioactive waste (Mohanty and McCartin, 2001), two approaches have been used to apply surface complexation modeling to describe actinide adsorption (Pabalan et al., 1998; Bertetti et al., 1998; Turner and Pabalan, 1999; Turner et al., 2002). One approach was to use a simplified DLM with available hydrochemistry data to provide realistic site-specific constraints on the probability density functions used in stochastic performance assessment codes to describe radionuclide adsorption. Specifically, for each separate groundwater analyses, values of pH and concentrations of the major cation and anion species were extracted from hydrochemistry databases; a DLM was used to establish mean, minimum, and maximum values for adsorption and related transport parameter probability density functions for sampling during a given TPA run. Correlation coefficients for multiple pairings of radioelements were also included as input into the TPA sampling routine, allowing the value selected for one radioelement adsorption parameter to be conditioned indirectly by its geochemical relationship to the other radioelements.

While using the DLM offline to constrain adsorption coefficient probability density functions is an approach that can be adapted quickly to current performance assessment approaches, it does not reduce the number of sampled parameters. Also, while the approach represents the effects of variable geochemical conditions on adsorption, it does not represent variation in a spatial sense. An alternative method that is being explored for incorporation into the TPA code is to use the DLM over a wide range of pH and pCO_2 conditions to develop an adsorption response surface as a function of geochemistry (Turner et al., 2002). During a given TPA realization, probability density functions for pH and pCO_2 are sampled, and the values used to determine the appropriate value for K_d from the response surface, either through a parametric representation of the surface or through interpolation of a look-up table.

Conclusions

The use of equilibrium geochemical models to calculate the solubilities and aqueous speciation of contaminants is well established in the field of geochemical modeling. Surface complexation modeling is an extension of this thermodynamic modeling approach to include the reactions between dissolved species and the functional groups present on mineral surfaces. The adsorption reactions are included as part of the network of chemical reactions that require equilibration, rather than as a condition-dependent partitioning coefficient, like K_d. Once the model is calibrated, it may allow predictive calculations for a range of geochemical conditions without changing the values of the stability constants for ion adsorption. The adsorption equations can be included efficiently in transport simulations where there are chemical gradients in the subsurface environment rather than constant chemical conditions (Curtis et al., 2006; Kent et al., 2000). This type of model also provides a more sound thermodynamic basis from which to examine uncertainty in transport parameters resulting from spatial heterogeneity in the physical and chemical characteristics of the system of interest.

The challenge in applying the surface complexation concept in the environment is to simplify the adsorption model, such that predicted adsorption is still calculated with mass laws that are coupled with aqueous speciation, while lumping parameters that are difficult to characterize in the environment with other parameters. To be applied by solute transport modelers and within risk assessment applications, the complexity of the adsorption model needs to be balanced with the goal of using the simplest possible model that is consistent with observed data. This can sometimes be achieved using the semi-empirical GC modeling approach (Kent et al., 2000; Davis and Curtis, 2003; Curtis et al., 2006). The GC modeling approach is a compromise between the simple constant K_d approach and more complex thermodynamic surface speciation models that are presently difficult to apply to the environment. An important limitation of the GC approach is that adsorption predictions should not be extrapolated to conditions outside of the range for which data were collected for model calibration. However, a GC model can be useful for predictive calculations that interpolate within the range of chemical conditions studied.

Historically, solute transport modelers have lacked the necessary expertise to apply the SCM approach, and many have believed that the models were too complex to be applied. While it is true that the most complex models are difficult to apply at present, it has been demonstrated that the simpler GC modeling approach can be applied to simulations of contaminant transport at the field scale. The GC modeling approach is preferable to completely empirical approaches, such as the constant K_d model or adsorption isotherms, because the important linkage between surface and aqueous species (and associated thermodynamic data) is retained through the coupling of mass action equations. This linkage also provides a framework for conducting uncertainty analyses based on process level parameters rather than on ranges of K_d values resulting from lumping together multiple

processes. The current operational paradigm that employs constant K_d values to describe retardation at the field scale introduces more uncertainty than necessary. This uncertainty can be reduced and more completely understood in the future using SCM modeling approaches.

Acknowledgments

The work of Kirk J. Cantrell and Louise J. Criscenti was primarily supported by the U.S. Nuclear Regulatory Commission (NRC), Office of Nuclear Regulatory Research. Kirk J. Cantrell gratefully acknowledges the guidance of NRC project manager, Tom Nicholson. Louise J. Criscenti is very grateful for the advice and support provided by NRC program manager, Edward O'Donnell, during the funding period. Additional support from the USDOE, Office of Basic Energy Sciences, Division of Chemical Sciences, Geosciences, and Biosciences and Office of Biological and Environmental Research is also greatly appreciated. Sandia National Laboratories is a multiprogram laboratory operated by the Sandia Corporation, a Lockheed Martin Company for the USDOE's National Nuclear Security Administration under Contract DE-AC04-94AL85000. Contributions to this paper by David R. Turner were prepared to document work performed by the Center for Nuclear Regulatory Analyses (CNWRA) for the NRC under Contract No. 02-03-004. These contributions are an independent product of the CNWRA and do not necessarily reflect the views or regulatory position of the NRC.

References

Allison, J.D., D.S. Brown, and K.J. Novo-Gradac. 1990. MINTEQA2/PRODEFA2—A geochemical assessment model for environmental systems: Version 3.0 user's manual. USEPA, Environmental Research Laboratory, Office of Research and Development, Athens, GA.

Allison Geoscience Consultants and Hydrogeologic. 2003. MINTEQA2 for Windows equilibrium speciation model: Version 1.5 users manual, Flowery Branch, GA.

Altmann, S.A., J. Bruno, and C. Tweed. 2001. Using thermodynamic sorption models for guiding radioelement distribution coefficient (K_d) investigations for performance assessment: A status report. Nuclear Energy Agency, Paris, France.

Ames, L.L., and D. Rai. 1978. Radionuclide interactions with rock and soil media. Vol. 1. USEPA 520/6-78-007-a. USEPA, Las Vegas, NV.

Anderson, M.A., and D.T. Malotky. 1979. The adsorption of protolyzable anions on hydrous oxides at the isoelectric point. J. Colloid Interface Sci. 72:413–427.

Anderson, M.A., J.F. Ferguson, and J. Gavis. 1976. Arsenate adsorption on amorphous aluminum hydroxide. J. Colloid Interface Sci. 54:391–399.

Andersson, K. 1998. SKI project-90: Chemical data. SKI Technical Report 91:21. Swedish Nuclear Power Inspectorate, Stockholm, Sweden.

Arai, Y., E.J. Elzinga, and D.L. Sparks. 2001. X-ray absorption spectroscopic investigation of arsenite and arsenate adsorption at the aluminum oxide-water interface. J. Colloid Interface Sci. 235:80–88.

Arai, Y., M. McBeath, J.R. Bargar, J. Joye, and J.A. Davis. 2006. Uranyl adsorption and surface speciation at the imogolite-water interface: Self-consistent spectroscopic and surface complexation models. Geochim. Cosmochim. Acta 70:2492–2509.

Arai, Y., D.L. Sparks, and J.A. Davis. 2004. Effects of dissolved carbonate on arsenate adsorption and surface speciation at the hematite-water interface. Environ. Sci. Technol. 38:817–824.

Arai, Y., D.L. Sparks, and J.A. Davis. 2005. Arsenate adsorption mechanisms at the allophane–water interface. Environ. Sci. Technol. 39:2537–2544.

Arnold, T., T. Zorn, H. Zanker, G. Bernhard, and H. Nitsche. 2001. Sorption behavior of U(VI) on phyllite: Experiments and modeling. J. Contam. Hydrol. 47:219–231.

Baes, C.F., and R.D. Sharp. 1983. A proposal for estimation of soil leaching and leaching constants for use in assessment models. J. Environ. Qual. 12:17–28.

Barber, L.B. 1994. Sorption of chlorobenzenes to Cape Cod aquifer sediments. Environ. Sci. Technol. 28:890–897.

Bargar, J.R., G.E. Brown, and G.A. Parks. 1997a. Surface complexation of Pb(II) at oxide–water interfaces: I. XAFS and bond-valence determination of mononuclear and polynuclear Pb(II) sorption products on aluminum oxides. Geochim. Cosmochim. Acta 61:2617–2637.

Bargar, J.R., G.E. Brown, and G.A. Parks. 1997b. Surface complexation of Pb(II) at oxide–water interfaces: II. XAFS and bond-valence determination of mononuclear and polynuclear Pb(II) sorption products on iron oxides. Geochim. Cosmochim. Acta 61:2639–2652.

Bargar, J.R., G.E. Brown, and G.A. Parks. 1998. Surface complexation of Pb(II) at oxide–water interfaces: III. XAFS and bond-valence determination of Pb(II) and Pb(II)-chloro adsorption complexes on goethite and alumina. Geochim. Cosmochim. Acta 62:193–207.

Bargar, J.R., R. Reitmeyer, J.J. Lenhart, and J.A. Davis. 2000. Characterization of U(VI)-carbonato ternary complexes on hematite: EXAFS and electrophoretic mobility measurements. Geochim. Cosmochim. Acta 64:2737–2749.

Bargar, J.R., S.N. Towle, G.E. Brown, and G.A. Parks. 1996. Outer-sphere Pb(II) adsorbed at specific surface sites on single crystal α-alumina. Geochim. Cosmochim. Acta 60:3541–3547.

Bargar, J.R., S.N. Towle, G.E. Brown, and G.A. Parks. 1997c. XAFS and bond-valence determination of the structures and compositions of surface functional groups and Pb(II) and Co(II) sorption products on single-crystal γ-Al_2O_3. J. Colloid Interface Sci. 185:473–492.

Benjamin, M.M. 2002. Modeling the mass-action expression for bidentate adsorption. Environ. Sci. Technol. 36:307–313.

Bertetti, F.P., R.T. Pabalan, and M.G. Almendarez. 1998. Studies of neptunium^{V} sorption on quartz, clinoptilolite, montmorillonite, and α-alumina. p. 131–148. *In* E.A. Jenne (ed.) Adsorption of metals by geomedia: Variables, mechanisms, and model applications. Proc. Am. Chem. Soc. Symp. Academic Press, San Diego, CA.

Bethke, C.M., and P.V. Brady. 2000. How the K_d approach undermines ground water cleanup. Ground Water 38:435–443.

Bleam, W.F., P.E. Pfeffer, S. Goldberg, R.W. Taylor, and R. Dudley. 1991. A ^{31}P solid-state nuclear magnetic resonance study of phosphate adsorption at the boehmite/aqueous-solution interface. Langmuir 7:1702–1712.

Boekhold, A.E., and S.E.A.T.M. van der Zee. 1992. A scaled sorption model validated at the column scale to predict cadmium contents in a spatially-variable field soil. Soil Sci. 154:105–112.

Borkovec, M., U. Rusch, and J.C. Westall. 1998. Modeling of competitive ion binding to heterogeneous materials with affinity distributions. p. 467–482. *In* E.A. Jenne (ed.) Adsorption of metals by geomedia: Variables, mechanisms, and model applications. Proc. Am. Chem. Soc. Symp., Academic Press, San Diego, CA.

Bosma, W.J.P., A. Bellin, S.E.A.T.M. van der Zee, and A. Rinaldo. 1993. Linear equilibrium adsorbing solute transport in physically and chemically heterogeneous porous formations: 2. Numerical results. Water Resour. Res. 29:4031–4043.

Bostick, B.C., M.A. Vairavamurthy, K.G. Karthikeyan, and J. Chorover. 2002. Cesium adsorption on clay minerals: An EXAFS spectroscopic investigation. Environ. Sci. Technol. 36:2670–2676.

Boyle-Wight, E.J., L.E. Katz, and K.F. Hayes. 2002. Spectroscopic studies of the effects of selenate and selenite on cobalt sorption to γ-Al_2O_3. Environ. Sci. Technol. 36:1219–1225.

Brady, P.V., B.P. Spalding, K.M. Krupka, R.D. Waters, P.-C. Zhang, D.J. Borns, and W.D. Brady. 1999. Site screening and technical guidance for monitored natural attenuation at DOE sites. SAND99-0464. Sandia National Laboratories, Albuquerque, NM.

Brendler, V., A. Richter, C. Nebelung, and A. Vahle. 2004. Development of a mineral specific sorption database for surface complexation modeling. Project PtWt+E 02E9471. FZ Rossendorf, e.V. Dresden, Germany.

Brendler, V., A. Vahle, T. Arnold, G. Bernhard, and T. Fanghaenel. 2003. RES^{3}T: Rossendorf expert system for surface and sorption thermodynamics. J. Contam. Hydrol. 61:281–291.

Brown, G.E. 1990. Spectroscopic studies of chemisorption reaction mechanisms at oxide–water interfaces. Rev. Mineral. 23:309–363.

Brown, G.E., G.A. Parks, and C.J. Chisholm-Brause. 1989. In-situ X-ray absorption spectroscopic studies of ions at oxide–water interfaces. Chimia (Aarau) 43:248–256.

Brown, G.E., G.A. Parks, and P.A. O'Day. 1995. Sorption at mineral–water interfaces: Macroscopic and microscopic perspectives. p. 129–183. *In* D.J. Vaughan and R.A.D. Pattrick (ed.) Mineral surfaces. Mineralogical Society Ser. 5. Chapman & Hill, New York.

Brown, I.D., and K.K. Altermatt. 1976. Bond-valence parameters obtained from a systematic analysis of the inorganic crystal-structure database. Acta Crystallogr. B41:244–247.

Brown, J.G., R.L. Bassett, and P.D. Glynn. 1998. Analysis and simulation of reactive transport of metal contaminants in ground water in Pinal Creek basin, Arizona. J. Hydrol. 209:225–250.

Brusseau, M.L., and R. Srivastava. 1999. Nonideal transport of reactive solutes in heterogeneous porous media: 4. Analysis of the Cape Cod natural-gradient field experiment. Water Resour. Res. 35:1113–1125.

Brusseau, M.L., and J.M. Zachara. 1993. Transport of Co^{2+} in a physically and chemically heterogeneous porous medium. Environ. Sci. Technol. 27:1937–1939.

Buergisser, C., M. Cernik, M. Borkovec, and H. Sticher. 1993. Determination of nonlinear adsorption isotherms from column experiments: An alternative to batch studies. Environ. Sci. Technol. 27:943–948.

Burr, D.T., E.A. Sudicky, and R.L. Naff. 1994. Nonreactive and reactive solute transport in 3-dimensional heterogeneous porous-media: Mean displacement, plume spreading, and uncertainty. Water Resour. Res. 30:791–815.

Cameron, D.R., and A. Klute. 1977. Convective–dispersive solute transport with a combined equilibrium and kinetic adsorption model. Water Resour. Res. 13:183–188.

Cantrell, K.J., R.J. Serne, and G.L. Last. 2003. Hanford contaminant distribution coefficient database and users guide. PNNL-13895, Rev. 1. Pacific Northwest National Laboratory, Richland, WA.

Cernik, M., P. Federer, M. Borkovec, and H. Sticher. 1994. Modeling of heavy-metal transport in a contaminated soil. J. Environ. Qual. 23:1239–1248.

Cheah, S.F., G.E. Brown, and G.A. Parks. 1998. XAFS spectroscopy study of Cu(II) sorption on amorphous SiO_2 and γ-Al_2O_3: Effect of substrate and time on sorption complexes. J. Colloid Interface Sci. 208:110–128.

Chen, C.-C., M.L. Coleman, and L.E. Katz. 2006. Bridging the gap between macroscopic and spectroscopic studies of metal ion sorption at the oxide/water interface: Sr(II), Co(II), and Pb(II) sorption to quartz. Environ. Sci. Technol. 40:142–148.

Chen, C.C., and K.F. Hayes. 1999. X-ray absorption spectroscopy investigation of aqueous Co(II) and Sr(II) sorption at clay-water interfaces. Geochim. Cosmochim. Acta 63:3205–3215.

Chen, C.C., C. Papelis, and K.F. Hayes. 1998. Extended X-ray absorption fine structure (EXAFS) analysis of aqueous Sr^{II} ion sorption at clay-water interfaces. p. 333–348. *In* E.A. Jenne (ed.) Adsorption of metals by geomedia: Variables, mechanisms, and model applications. Proc. Am. Chem. Soc. Symp. Academic Press, San Diego, CA.

Chisholm-Brause, C.J., J.M. Berg, R.A. Matzner, and D.E. Morris. 2001. Uranium(VI) sorption complexes on montmorillonite as a function of solution chemistry. J. Colloid Interface Sci. 233:38–49.

Chisholm-Brause, C.J., K.F. Hayes, A.L. Roe, G.E. Brown, G.A. Parks, and J.O. Leckie. 1990a. Spectroscopic investigation of Pb(II) complexes at the γ-Al_2O_3/water interface. Geochim. Cosmochim. Acta 54:1897–1909.

Chisholm-Brause, C.J., P.A. O'Day, G.E. Brown, and G.A. Parks. 1990b. Evidence for multinuclear metal-ion complexes at solid/water interfaces from X-ray absorption spectroscopy. Nature 348:528–531.

Christensen, T.H. 1985. Cadmium soil sorption at low concentrations: 3. Prediction and observation of mobility. Water Air Soil Pollut. 26:255–264.

Civilian Radioactive Waste Management System Management and Operating Contractor. 1998. Total system performance assessment: Viability assessment (TSPA-VA) analyses technical basis document. B00000000-01717-4301. Rev. 01. CRWMS M&O, Las Vegas, NV.

Civilian Radioactive Waste Management System Management and Operating Contractor. 2000a. Total system performance assessment for the site recommendation. TDF-WIS-PA-00001. Rev. 00 ICN 01. CRWMS M&O, Las Vegas, NV.

Civilian Radioactive Waste Management System Management and Operating Contractor. 2000b. Total system performance assessment (TSPA) model for site recommendation. MDL-WIS-PA-000002. Rev. 00. CRWMS M&O, Las Vegas, NV.

Collins, C.R., D.M. Sherman, and K.V. Ragnarsdóttir. 1998. The adsorption mechanism of Sr^{2+} on the surface of goethite. Radiochim. Acta 81:201–206.

Collins, C.R., D.M. Sherman, and K.V. Ragnarsdóttir. 1999. Surface complexation of Hg^{2+} on goethite: Mechanism from EXAFS spectroscopy and density functional calculations. J. Colloid Interface Sci. 219:345–350.

Coston, J.A., C.C. Fuller, and J.A. Davis. 1995. Pb^{2+} and Zn^{2+} adsorption by a natural aluminum and iron bearing surface coating on an aquifer sand. Geochim. Cosmochim. Acta 59:3535–3547.

Criscenti, L.J., and D.A. Sverjensky. 1999. The role of electrolyte anions (ClO_4^-, NO_3^-, Cl^-) in divalent metal (M^{2+}) adsorption on oxide and hydroxide surfaces in salt solutions. Am. J. Sci. 299:828–899.

Criscenti, L.J., and D.A. Sverjensky. 2002. A single-site model for divalent transition and heavy metal adsorption over a range of metal concentrations. J. Colloid Interface Sci. 253:329–352.

Curtis, G.P., J.A. Davis, and D.L. Naftz. 2006. Simulation of reactive transport of uranium(VI) in groundwater with variable chemical conditions. Water Resour. Res. 42:W04404, doi:10.1029/2005WR003979.

Dähn, R., A.M. Scheidegger, A. Manceau, M.L. Schlegel, B. Baeyens, M.H. Bradbury, and D. Chateigner. 2003. Structural evidence for the sorption of Ni(II) atoms on the edges of montmorillonite clay minerals: A polarized X-ray absorption fine structure study. Geochim. Cosmochim. Acta 67:1–15.

Davis, J.A. 2001. Surface complexation modeling of uranium(VI) adsorption on natural mineral assemblages. NUREG/CR-6708. U.S. Nuclear Regulatory Commission, Washington, DC.

Davis, J.A., J.A. Coston, D.B. Kent, and C.C. Fuller. 1998. Application of the surface complexation concept to complex mineral assemblages. Environ. Sci. Technol. 32:2820–2828.

Davis, J.A., and G.P. Curtis. 2003. Application of surface complexation modeling to describe uranium(VI) adsorption and retardation at the uranium mill tailings site at Naturita, Colorado. NUREG/CR-6820. U.S. Nuclear Regulatory Commission, Washington, DC.

Davis, J.A., R.O. James, and J.O. Leckie. 1978. Surface ionization and complexation at the oxide/water interface: 1. Computation of electrical double layer properties in simple electrolytes. J. Colloid Interface Sci. 63:480–499.

Davis, J.A., and D.B. Kent. 1990. Surface complexation modeling in aqueous geochemistry. Rev. Mineral. 23:177–260.

Davis, J.A., D.E. Meece, M. Kohler, and G.P. Curtis. 2004a. Approaches to surface complexation modeling of uranium(VI) adsorption on aquifer sediments. Geochim. Cosmochim. Acta 68:3621–3641.

Davis, J.A., M. Ochs, M. Olin, T.E. Payne, and C.J. Tweed. 2005. Interpretation and prediction of radionuclide sorption onto substrates relevant for radioactive waste disposal using thermodynamic sorption models. NEA Sorption Project, Phase II, NEA Report 5992. OECD, Paris, France.

Davis, J.A., T.E. Payne, and T.D. Waite. 2002. Simulating the pH and pCO_2 dependence of uranium(VI) adsorption by a weathered schist with surface complexation models. p. 61–86. *In* P.-C. Zhang and P.V. Brady (ed.) Geochemistry of soil radionuclides. SSSA Special Pub. 59. SSSA, Madison, WI.

Davis, J.A., S.B. Yabusaki, C.I. Steefel, J.M. Zachara, G.P. Curtis, G.D. Redden, L.J. Criscenti, and B.D. Honeyman. 2004b. Assessing conceptual models for subsurface reactive transport of inorganic contaminants. Eos 85:449–455.

Dyer, J.A., P. Trivedi, N.C. Scrivner, and D.L. Sparks. 2003. Lead sorption onto ferrihydrite: 2. Surface complexation modeling. Environ. Sci. Technol. 37:915–922.

Dzombak, D.A., and M.A. Ali. 1993. Hydrochemical modeling of metal fate and transport in freshwater environments. Water Pollut. Res. J. Can. 28:7–50.

Dzombak, D.A., and F.M.M. Morel. 1990. Surface complexation modeling: Hydrous ferric oxide. John Wiley & Sons, New York.

Felmy, A.R., and J.R. Rustad. 1998. Molecular statics calculations of proton binding to goethite surfaces: Thermodynamic modeling of the surface charging and protonation of goethite in aqueous solution. Geochim. Cosmochim. Acta 62:25–31.

Fendorf, S.E., M.J. Eick, P. Grossl, and D.L. Sparks. 1997. Arsenate and chromate retention mechanisms on goethite: I. Surface structure. Environ. Sci. Technol. 31:315–320.

Fendorf, S.E., G.M. Lamble, M.G. Stapleton, M.J. Kelley, and D.L. Sparks. 1994. Mechanisms of chromium (III) sorption on silica: 1. Cr(III) surface structure derived by extended X-ray absorption fine structure spectroscopy. Environ. Sci. Technol. 28:284–289.

Fenter, P., L. Cheng, S. Rihs, M.L. Machesky, M.J. Bedzyk, and N.C. Sturchio. 2000. Electrical double-layer structure at the rutile-water interface as observed in situ with small-period X-ray standing waves. J. Colloid Interface Sci. 225:154–165.

Freeze, R.A., and J.A. Cherry. 1979. Groundwater. Prentice Hall, Englewood Cliffs, NJ.

Friedly, J.C., J.A. Davis, and D.B. Kent. 1995. Modeling hexavalent chromium

seduction in groundwater in field-scale transport and laboratory batch experiments. Water Resour. Res. 31:2783–2794.
Freundlich, H. 1926. Colloid and capillary chemistry. Methuen, London.
Fuller, C.C., J.A. Davis, J.A. Coston, and E. Dixon. 1996. Characterization of metal adsorption variability in a sand and gravel aquifer, Cape Cod, Massachusetts, USA. J. Contam. Hydrol. 22:165–187.
Garabedian, S.P., D.R. LeBlanc, L.W. Gelhar, and M.A. Celia. 1991. Large-scale natural gradient tracer test in sand and gravel, Cape Cod, Massachusetts: 2. Analysis of spatial moments for a nonreactive tracer. Water Resour. Res. 27:911–924.
Gee, G.W., A.C. Campbell, D.R. Sherwood, R.G. Strickert, and S.J. Phillips. 1980. Interaction of uranium mill tailings leachate with soils and clay liners. NUREG CR-1494, PNL-3381 Prepared by Pacific Northwest Laboratory, Richland, WA, for Office of Nuclear Regulatory Research, U.S. Nuclear Regulatory Commission, Washington, DC.
Gelhar, L.W., and C.L. Axness. 1983. 3-dimensional stochastic-analysis of macrodispersion in aquifers. Water Resour. Res. 19:161–180.
Goldberg, S. 1991. Sensitivity of surface complexation modeling to the surface site density parameter. J. Colloid Interface Sci. 145:1–9.
Goldberg, S. 1999. Reanalysis of boron adsorption on soils and soil minerals using the constant capacitance model. Soil Sci. Soc. Am. J. 63:823–829.
Goldberg, S. 2004. Modeling boron adsorption isotherms and envelopes using the constant capacitance model. www.vadosezonejournal.org. Vadose Zone J. 3:676–680.
Goldberg, S., D.L. Corwin, P.J. Shouse, and D.L. Suarez. 2005a. Prediction of boron adsorption by field samples of diverse textures. Soil Sci. Soc. Am. J. 69:1379–1388.
Goldberg, S., H.S. Forster, and C.L. Godfrey. 1996. Molybdenum adsorption on oxides, clay minerals, and soils. Soil Sci. Soc. Am. J. 60:425–432.
Goldberg, S., H.S. Forster, and E.L. Heick. 1993. Boron adsorption mechanisms on oxides, clay minerals, and soils inferred from ionic strength effects. Soil Sci. Soc. Am. J. 57:704–708.
Goldberg, S., and R.A. Glaubig. 1986. Boron adsorption on California soils. Soil Sci. Soc. Am. J. 50:1173–1176.
Goldberg, S., and R.A. Glaubig. 1988a. Anion sorption on a calcareous, montmorillonitic soil: Arsenic. Soil Sci. Soc. Am. J. 52:1297–1300.
Goldberg, S., and R.A. Glaubig. 1988b. Anion sorption on a calcareous, montmorillonitic soil: Selenium. Soil Sci. Soc. Am. J. 52:954–958.
Goldberg, S., and C.T. Johnston. 2001. Mechanisms of arsenic adsorption on amorphous oxides evaluated using macroscopic measurements, vibrational spectroscopy, and surface complexation modeling. J. Colloid Interface Sci. 234:204–216.
Goldberg, S., I. Lebron, D.L. Suarez, and Z.R. Hinedi. 2001. Surface characterization of amorphous aluminum oxides. Soil Sci. Soc. Am. J. 65:78–86.
Goldberg, S., S.M. Lesch, and D.L. Suarez. 2000. Predicting boron adsorption by soils using soil chemical parameters in the constant capacitance model. Soil Sci. Soc. Am. J. 64:1356–1363.
Goldberg, S., S.M. Lesch, and D.L. Suarez. 2002. Predicting molybdenum adsorption by soils using soil chemical parameters in the constant capacitance model. Soil Sci. Soc. Am. J. 66:1836–1842.
Goldberg, S., S.M. Lesch, D.L. Suarez, and N.T. Basta. 2005b. Predicting arsenate adsorption by soils using soil chemical parameters in the constant capacitance model. Soil Sci. Soc. Am. J. 69:1389–1398.
Goldberg, S., and G. Sposito. 1984. A chemical model of phosphate adsorption by soils: II. Noncalcareous soils. Soil Sci. Soc. Am. J. 48:779–783.
Goldberg, S., C. Su, and H.S. Forster. 1998. Sorption of molybdenum on oxides, clay minerals, and soils: Mechanisms and models. p. 401–426. *In* E.A. Jenne (ed.) Adsorption of metals by geomedia: Variables, mechanisms, and model applications. Proc. Am. Chem. Soc. Symp. Academic Press, San Diego, CA.
Goldberg, S., D.L. Suarez, N.T. Basta, and S.M. Lesch. 2004. Predicting boron adsorption isotherms by Midwestern soils using the constant capacitance model. Soil Sci. Soc. Am. J. 68:795–801.
Greaves, G.N. 1995. New X-ray techniques and approaches to surface mineralogy. p. 87–128. *In* D.J. Vaughan and R.A.D. Pattrick (ed.) Mineral surfaces. Mineralogical Society Series 5. Chapman & Hill, New York.
Grenthe, I., J. Fuger, R.J.M. Konings, R.J. Lemire, A.J. Muller, C. Nguyen-Trung, and H. Wanner. 1992. Chemical thermodynamics of uranium. Elsevier, Amsterdam, the Netherlands.
Grossl, P.R., M. Eick, D.L. Sparks, S. Goldberg, and C.C. Ainsworth. 1997. Arsenate and chromate retention mechanisms on goethite: II. Kinetic evaluation using a pressure-jump relaxation technique. Environ. Sci. Technol. 31:321–326.
Guillaumont, R., T. Fanghanel, V. Neck, J. Fuger, D.A. Palmer, I. Grenthe, and M.H. Rand. 2003. Update on the chemical thermodynamics of uranium, neptunium, plutonium, americium, and technetium. Elsevier, Amsterdam, the Netherlands.
Harrison, J.B., and V.E. Berkheiser. 1982. Anion interactions with freshly prepared hydrous iron oxides. Clays Clay Miner. 30:97–102.
Hayes, K.F., and L.E. Katz. 1996. Application of X-ray absorption spectroscopy for surface complexation modeling of metal ion sorption. p. 147–223. *In* P.V. Brady (ed.) Physics and chemistry of mineral surfaces. CRC Press, Boca Raton, FL.
Hayes, K.F., and J.O. Leckie. 1986. Mechanism of lead ion adsorption at the goethite–water interface. Am. Chem. Soc. Symp. Ser. 323:114–141.
Hayes, K.F., and J.O. Leckie. 1987. Modeling ionic strength effects on cation adsorption at hydrous oxide/solution interfaces. J. Colloid Interface Sci. 115:564–572.
Hayes, K.F., C. Papelis, and J.O. Leckie. 1988. Modeling ionic strength effects on anion adsorption at hydrous oxide/solution interfaces. J. Colloid Interface Sci. 125:717–726.
Hayes, K.F., G. Redden, W. Ela, and J.O. Leckie. 1991. Surface complexation models: An evaluation of model parameter estimation using FITEQL and oxide mineral titration data. J. Colloid Interface Sci. 142:448–469.
Hayes, K.F., A.L. Roe, G.E. Brown, K.O. Hodgson, J.O. Leckie, and G.A. Parks. 1987. In situ X-ray absorption study of surface complexes: Selenium oxyanions on α-FeOOH. Science 238:783–786.
Herbelin, A.L., and J.C. Westall. 1999. FITEQL 4.0: A computer program for determination of chemical equilibrium constants from experimental data. Report 99-01. Dep. of Chemistry, Oregon State Univ., Corvallis.
Hess, K.M., S.H. Wolf, and M.A. Celia. 1992. Large-scale natural gradient tracer test in sand and gravel, Cape Cod, Massachusetts: 3. Hydraulic conductivity variability and calculated macrodispersivities. Water Resour. Res. 28:2011–2027.
Hiemstra, T., J.C.M. deWit, and W.H. van Riemsdijk. 1989a. Multisite proton adsorption modeling at the solid/solution interface on (hydr)oxides—A new approach: II. Application to various important (hydr)oxides. J. Colloid Interface Sci. 133:105–117.
Hiemstra, T., and W.H. van Riemsdijk. 1996. A surface structural approach to ion adsorption: The charge distribution (CD) model. J. Colloid Interface Sci. 179:488–508.
Hiemstra, T., and W.H. van Riemsdijk. 1999. Surface structural ion adsorption modeling of competitive binding of oxyanions by metal (hydr)oxides. J. Colloid Interface Sci. 210:182–193.
Hiemstra, T., W.H. van Riemsdijk, and G.H. Bolt. 1989b. Multisite proton adsorption modeling at the solid/solution interface of (hydr)oxides—A new approach: I. Model description and evaluation of intrinsic reaction constants. J. Colloid Interface Sci. 133:91–104.
Hiemstra, T., P. Venema, and W.H. van Riemsdijk. 1996. Intrinsic proton affinity of reactive surface groups of metal (hydr)oxides: The bond valence principle. J. Colloid Interface Sci. 184:680–692.
Higgins, G. 1959. Evaluation of the ground-water contamination hazard from underground nuclear explosions. J. Geophys. Res. 64:1509–1519.
Hinz, C., and H.M. Selim. 1994. Transport of zinc and cadmium in soils: Experimental evidence and modeling approaches. Soil Sci. Soc. Am. J. 58:1316–1327.
Honeyman, B.D. 1984. Cation and anion adsorption at the oxide/solution interface in systems containing binary mixtures of adsorbents: An investigation of the concept. Ph.D. diss. Stanford Univ., Stanford, CA.
Hsia, T.H., S.L. Lo, C.F. Lin, and D.Y. Lee. 1993. Chemical and spectroscopic evidence for specific adsorption of chromate on hydrous iron oxide. Chemosphere 26:1897–1904.
Hsia, T.H., S.L. Lo, C.F. Lin, and D.Y. Lee. 1994. Characterization of arsenate adsorption on hydrous iron oxide using chemical and physical methods. Colloids Surf., A Physicochem. Eng. Asp. 85:1–7.
Hug, S.J. 1997. In situ Fourier transform infrared measurements of sulfate adsorption on hematite in aqueous solutions. J. Colloid Interface Sci. 188:415–422.
Hunter, R.J. 1981. Zeta potential in colloid science: Principles and applications. Academic Press, London.
Isherwood, D. 1981. Geoscience data base handbook for modeling a nuclear

waste repository, NUREG/CR-0912. Vols. 1–2. U.S. Nuclear Regulatory Commission, Washington, DC.

Jacobs, L.A., H.R. von Gunten, R. Keil, and M. Kuslys. 1988. Geochemical changes along a river-groundwater infiltration flow path: Glattfelden, Switzerland. Geochim. Cosmochim. Acta 52:2693–2706.

James, R.O., and T.W. Healy. 1972a. Adsorption of hydrolyzable metal ions at the oxide–water interface: I. Co(II) adsorption on SiO_2 and TiO_2 as model systems. J. Colloid Interface Sci. 40:42–52.

James, R.O., and T.W. Healy. 1972b. Adsorption of hydrolyzable metal ions at the oxide–water interface: II. Charge reversal of SiO_2 and TiO_2 colloids by absorbed Co(II), La(III), and Th(IV) as model systems. J. Colloid Interface Sci. 40:53–64.

James, R.O., and T.W. Healy. 1972c. Adsorption of hydrolyzable metal ions at the oxide–water interface: III. A thermodynamic model of adsorption. J. Colloid Interface Sci. 40:65–81.

Katz, L.E., and K.F. Hayes. 1995. Surface complexation modeling: II. Strategy for modeling polymer and precipitation reactions at high surface coverage. J. Colloid Interface Sci. 170:491–501.

Kennedy, J.D., and D.L. Strenge. 1992. Residual radioactive contamination from decommissioning: Technical basis for translating contamination levels to annual total effective dose equivalent. NUREG CR-5512, PNL-7994 U.S. Nuclear Regulatory Commission, Washington, DC.

Kent, D.B., R.H. Abrams, J.A. Davis, J.A. Coston, and D.R. LeBlanc. 2000. Modeling the influence of variable pH on the transport of zinc in a contaminated aquifer using semiempirical surface complexation models. Water Resour. Res. 36:3411–3425.

Kinniburgh, D.G. 1986. General purpose adsorption isotherms. Environ. Sci. Technol. 20:895–904.

Kohler, M., G.P. Curtis, D.B. Kent, and J.A. Davis. 1996. Experimental investigation and modeling of uranium(VI) transport under variable chemical conditions. Water Resour. Res. 32:3539–3551.

Kohler, M., G.P. Curtis, D.E. Meece, and J.A. Davis. 2004. Methods for estimating adsorbed uranium(VI) and distribution coefficients of contaminated sediments. Environ. Sci. Technol. 38:240–247.

Kooner, Z.S., P.M. Jardine, and S. Feldman. 1995. Competitive surface complexation reactions of sulfate and natural organic carbon on soil. J. Environ. Qual. 24:656–662.

Koretsky, C. 2000. The significance of surface complexation reactions in hydrologic systems: A geochemist's perspective. J. Hydrol. 230:127–171.

Koretsky, C.M., D.A. Sverjensky, and N. Sahai. 1998. A model of surface site types on oxide and silicate minerals based on crystal chemistry: Implications for site types and densities, multi-site adsorption, surface infrared spectroscopy, and dissolution kinetics. Am. J. Sci. 298:349–438.

Kulik, D.A. 2000. Thermodynamic properties of surface species at the mineral–water interface under hydrothermal conditions: A Gibbs energy minimization single-site $2pK_A$ triple-layer model of rutile in NaCl electrolyte to 250 °C. Geochim. Cosmochim. Acta 64:3161–3179.

Kulik, D.A. 2002. Gibbs energy minimization approach to modeling sorption equilibria at the mineral-water interface: Thermodynamic relations for multi-site-surface complexation. Am. J. Sci. 302:227–279.

Ladeira, A.C.Q., V.S.T. Ciminelli, H.A. Duarte, M.C.M. Alves, and A.Y. Ramos. 2001. Mechanism of anion retention from EXAFS and density functional calculations: Arsenic(V) adsorbed on gibbsite. Geochim. Cosmochim. Acta 65:1211–1217.

Langmuir, D. 1918. The adsorption of gases on plane surfaces of glass, mica, and platinum. J. Am. Chem. Soc. 40:1361–1403.

Looney, B.B., M.W. Grant, and C.M. King. 1987. Estimation of geochemical parameters for assessing subsurface transport at the Savannah River plant. DPST-85-904. Savannah River Laboratory, Aiken, SC.

Lumsdon, D.G., A.R. Fraser, J.D. Russell, and N.T. Livesey. 1984. New infrared band assignments for the arsenate ion adsorbed on synthetic goethite (α-FeOOH). J. Soil Sci. 35:381–386.

Lützenkirchen, J., J.-F. Boily, L. Lövgren, and S. Sjöberg. 2002. Limitations of the potentiometric titration technique in determining the proton active site density of goethite surfaces. Geochim. Cosmochim. Acta 66:3389–3396.

Machesky, M.L., B.L. Bischoff, and M.A. Anderson. 1989. Calorimetric investigation of anion adsorption onto goethite. Environ. Sci. Technol. 23:580–587.

Machesky, M.L., and P.F. Jacobs. 1991a. Titration calorimetry of aqueous alumina suspensions: Part I. Results and comparisons with similar studies. Colloids Surf. 53:297–314.

Machesky, M.L., and P.F. Jacobs. 1991b. Titration calorimetry of aqueous alumina suspensions: Part II. Discussion of enthalpy changes with pH and ionic strength. Colloids Surf. 53:315–328.

Manceau, A., and L. Charlet. 1994. The mechanism of selenate adsorption on goethite and hydrous oxide. J. Colloid Interface Sci. 168:87–93.

Manceau, A., K.L. Nagy, L. Spadini, and K.V. Ragnarsdottir. 2000. Influence of anionic layer structure of Fe-oxyhydroxides on the structure of Cd surface complexes. J. Colloid Interface Sci. 228:306–316.

Manning, B.A., S.E. Fendorf, and S. Goldberg. 1998. Surface structures and stability of arsenic(III) on goethite: Spectroscopic evidence for inner-sphere complexes. Environ. Sci. Technol. 32:2383–2388.

Manning, B.A., and S. Goldberg. 1996. Modeling competitive adsorption of arsenate with phosphate and molybdate on oxide minerals. Soil Sci. Soc. Am. J. 60:121–131.

Mathur, S.S. 1995. Development of a database for ion sorption on goethite using surface complexation modeling. PhD. diss. Carnegie Mellon Univ., Pittsburgh, PA.

McBride, M.B. 1997. A critique of diffuse double layer models applied to colloid and surface chemistry. Clays Clay Miner. 45:598–608.

McBride, M.B., B.K. Richards, T. Steenhuis, H.J. Russo, and S. Sauve. 1997. Mobility and solubility of toxic metals and nutrients in soil fifteen years after sludge application. Soil Sci. 162:487–500.

McKenzie, R.M. 1983. The adsorption of molybdenum on oxide surfaces. Aust. J. Soil Res. 21:505–513.

McKinley, I.G., and A. Scholtis. 1991. Compilation and comparison of radionuclide sorption databases used in recent performance assessments. p. 21–55. *In* Radionuclide sorption from the safety evaluation perspective. Proc. of an NEA Workshop, Interlaken, Switzerland. 16–18 Oct. 1991. OECD, Paris, France.

Meeussen, J.C.L., A. Scheidegger, T. Hiemstra, W.H. van Riemsdijk, and M. Borkovec. 1996. Predicting multicomponent adsorption and transport of fluoride at variable pH in a goethite–silica sand system. Environ. Sci. Technol. 30:481–488.

Middleburg, J.J., and R.N.J. Comans. 1991. Sorption of cadmium on hydroxyapatite. Chem. Geol. 90:45–53.

Mohanty, S., and T.J. McCartin. 2001. NRC sensitivity and uncertainty analyses for a proposed HLW repository at Yucca Mountain, Nevada: Using TPA 3.1. NUREG-1668. Vol. 1. U.S. Nuclear Regulatory Commission, Washington, DC.

Morin, K.A., J.A. Cherry, T.P. Lim, and A.J. Vivyurka. 1982. Contaminant migration in a sand aquifer near an inactive uranium tailings impoundment, Elliot Lake, Ontario. Can. Geotech. J. 19:49–62.

Moyes, L.N., R.H. Parkman, J.M. Charnock, D.J. Vaughan, F.R. Livens, C.R. Hughes, and A. Braithwaite. 2000. Uranium uptake from aqueous solution by interaction with goethite, lepidocrocite, muscovite, and mackinawite: An X-ray absorption spectroscopy study. Environ. Sci. Technol. 34:1062–1068.

Nuclear Safety Associates. 1980. Comparison of alternatives for long-term management of high-level radioactive waste at the western New York Nuclear Service Center, Appendix IIIC. Nuclear Safety Associates, Bethesda, MD.

O'Day, P.A., G.E. Brown, and G.A. Parks. 1994a. Absorption spectroscopy of cobalt(II) multinuclear surface complexes and surface precipitates on kaolinite. J. Colloid Interface Sci. 165:269–289.

O'Day, P.A., C.J. Chisholm-Brause, S.N. Towle, G.A. Parks, and G.E. Brown. 1996. X-ray absorption spectroscopy of Co(II) sorption complexes on quartz (α-SiO_2) and rutile (TiO_2). Geochim. Cosmochim. Acta 60:2515–2532.

O'Day, P.A., G.A. Parks, and G.E. Brown. 1994b. Molecular structure and binding sites of cobalt(II) surface complexes on kaolinite from X-ray absorption spectroscopy. Clays Clay Miner. 42:337–355.

O'Day, P.A., M. Newville, P.S. Neuhoff, N. Sahai, and S.A. Carroll. 2000. X-ray absorption spectroscopy of strontium (II) coordination: I. Static and thermal disorder in crystalline, hydrated, and precipitated solids and in aqueous solution. J. Colloid Interface Sci. 222:184–197.

Pabalan, R.T., and D.R. Turner. 1996. Uranium(6+) sorption on montmorillonite: Experimental and surface complexation modeling study. Aquat. Geochem. 2:203–226.

Pabalan, R.T., D.R. Turner, F.P. Bertetti, and J.D. Prikryl. 1998. Uranium^{VI} sorption onto selected mineral surfaces: Key geochemical parameters. p. 99–130. *In* E.A. Jenne (ed.) Adsorption of metals by geomedia: Variables,

mechanisms, and model applications. Proc. Am. Chem. Soc. Symp. Academic Press, San Diego, CA.

Painter, S., V. Cvetkovic, and D.R. Turner. 2001. Effect of heterogeneity on radionuclide retardation in the alluvial aquifer near Yucca Mountain. Ground Water 39:326–338.

Parkhurst, D.L., and C.A.J. Appelo. 1999. User's guide to PHREEQC (Version 2): A computer program for speciation, batch-reaction, one-dimensional transport, and inverse geochemical calculations. USGS Water Resources Investigations Report 99-4259. USGS, Denver, CO.

Payne, T.E., J.A. Davis, M. Ochs, M. Olin, and C.J. Tweed. 2004. Uranium adsorption on weathered schist: Intercomparison of modelling approaches. Radiochim. Acta 92:651–661.

Peak, D., R.G. Ford, and D.L. Sparks. 1999. An in situ ATR-FTIR investigation of sulfate bonding mechanisms on goethite. J. Colloid Interface Sci. 218:289–299.

Peak, D., and D.L. Sparks. 2002. Mechanisms of selenate adsorption on iron oxides and hydroxides. Environ. Sci. Technol. 36:1460–1466.

Persson, P., N. Nilsson, and S. Sjöberg. 1996. Structure and bonding of orthophosphate ions at the iron oxide-aqueous interface. J. Colloid Interface Sci. 177:263–275.

Pickens, J.F., R.E. Jackson, K.J. Inch, and W.F. Merritt. 1981. Measurement of distribution coefficients using a radial injection dual-tracer test. Water Resour. Res. 17:529–544.

Pierce, M.L., and C.B. Moore. 1980. Adsorption of arsenite on amorphous iron hydroxide from dilute aqueous solution. Environ. Sci. Technol. 14:214–216.

Randall, S.R., D.M. Sherman, K.V. Ragnarsdottir, and C.R. Collins. 1999. The mechanism of cadmium surface complexation on iron oxyhydroxide minerals. Geochim. Cosmochim. Acta 63:2971–2987.

Ravat, C., J. Dumonceau, and F. Monteil-Rivera. 2000. Acid/base and Cu(II) binding properties of natural organic matter extracted from wheat bran: Modeling by the surface complexation model. Water Res. 34:1327–1339.

Reardon, E.J. 1981. K_d's: Can they be used to describe reversible ion sorption reactions in contaminant migration? Ground Water 19:279–286.

Richter, A., V. Brendler, and G. Bernhard. 2003. The mineral-specific thermodynamic sorption database RES^{3}T: Concept description, implementation, and application towards contaminated systems. Geochim. Cosmochim. Acta Supp. 67:397.

Robin, J.J.L., E.A. Sudicky, R.W. Gillham, and R.G. Kachanoski. 1991. Spatial variability of strontium distribution coefficients and their correlation with hydraulic conductivity in the Canadian Forces Base Borden aquifer. Water Resour. Res. 27:2619–2632.

Rosentreter, J.J., H.S. Quarder, R.W. Smith, and T. McLing. 1998. Uranium sorption onto natural sands as a function of sediment characteristics and pH. p. 181–192. *In* E.A. Jenne (ed.) Adsorption of metals by geomedia: Variables, mechanisms, and model applications. Proc. Am. Chem. Soc. Symp. Academic Press, San Diego, CA.

Routson, R.C., and R.J. Serne. 1972. Experimental support studies for the PERCOL and transport models. USAEC Report BNWL-1719. Pacific Northwest Laboratory, Richland, WA.

Rüegger, B., and K.V. Ticknor. 1992. The NEA sorption data base (SDB): Radionuclide sorption from the safety evaluation perspective. p. 57–78. *In* Proc. of a Nuclear Energy Agency Workshop, Interlaken, Switzerland, 16–18 October 1991. OECD, Paris, France.

Sahai, N., S.A. Carroll, S. Roberts, and P.A. O'Day. 2000. X-ray absorption spectroscopy of strontium(II) coordination: II. Sorption and precipitation at kaolinite, amorphous silica, and goethite surfaces. J. Colloid Interface Sci. 222:198–212.

Sahai, N., and D.A. Sverjensky. 1997a. Evaluation of internally consistent parameters for the triple layer model by the systematic analysis of oxide surface titration data. Geochim. Cosmochim. Acta 61:2801–2826.

Sahai, N., and D.A. Sverjensky. 1997b. Solvation and electrostatic model for specific electrolyte adsorption. Geochim. Cosmochim. Acta 61:2827–2848.

Sauve, S., W. Hendershot, and H.E. Allen. 2000. Solid–solution partitioning of metals in contaminated soils: Dependence on pH, total metal burden, and organic matter. Environ. Sci. Technol. 34:1125–1131.

Scheidegger, A., C.S. Buergisser, M. Borkovec, H. Stricher, H. Meeusen, and W. van Riemsdijk. 1994. Convective-transport of acids and bases in porous-media. Water Resour. Res. 30:2937–2944.

Scheidegger, A.M., M. Fendorf, and D.L. Sparks. 1996. Mechanisms of nickel sorption on pyrophyllite: Macroscopic and microscopic approaches. Soil Sci. Soc. Am. J. 60:1763–1772.

Scheidegger, A.M., G.M. Lamble, and D.L. Sparks. 1997. Spectroscopic evidence for the formation of mixed-cation hydroxide phases upon metal sorption on clays and aluminum oxides. J. Colloid Interface Sci. 186:118–128.

Scheidegger, A.M., D.G. Strawn, G.M. Lamble, and D.L. Sparks. 1998. The kinetics of mixed Ni-Al hydroxide formation on clay and aluminum oxide minerals: A time-resolved XAFS study. Geochim. Cosmochim. Acta 62:2233–2245.

Scheinost, A.C., and D.L. Sparks. 2000. Formation of layered single- and double-metal hydroxide precipitates at the mineral/water interface: A multiple-scattering XAFS analysis. J. Colloid Interface Sci. 223:167–178.

Selim, H.M., J.M. Davidson, and R.S. Mansell. 1976. Evaluation of a 2-site adsorption–desorption model for describing solute transport in soils. p. 444–448. *In* Proc. 1976 Summer Computer Simulation Conf. Simulation Councils, La Jolla, CA.

Serne, R.J., R.C. Routson, and D.A. Cochran. 1974. Experimental methods for obtaining PERCOL model input and verification data. BNWL-1721. Battelle Pacific Northwest Labs., Richland, WA.

Sheppard, M.L., S.C. Sheppard, and B.D. Amiro. 1991. Mobility and plant uptake of inorganic ^{14}C and ^{14}C-labeled PCB in soils of high and low retention. Health Phys. 61:481–492.

Sheppard, M.L., and D.H. Thibault. 1990. Default soil solid/liquid partition coefficients, K_ds, for four major soil types: A compendium. Health Phys. 59:471–478.

Siegel, M.D., R. Rechard, K.L. Erickson, J.O. Leckie, D.B. Kent, D.A. Grover, S. Philips, R. Guzowski, and S. Faith. 1989. Progress in development of a methodology for geochemical sensitivity analysis for performance assessment. Vol. 2. Speciation, sorption, and transport in fractured media. Project NRC FIN A1756. Letter Report to NRC. Division of High Level Waste Management, Office of Nuclear Regulatory Research, Washington, DC.

Silva, R.J., G. Bidoglio, M.H. Rand, P.B. Robouch, H. Wanner, and I. Puigdomenech. 1995. Chemical thermodynamics of Americium, with an appendix on chemical thermodynamics of uranium. Nuclear Energy Agency, OECD, Elsevier, North-Holland, the Netherlands.

Smith, R.M., and A.E. Martell. 1989. Critical stability constants. Plenum, New York.

Smith, R.W., and E.A. Jenne. 1991. Recalculation, evaluation, and prediction of surface complexation constants for metal adsorption on iron and manganese oxides. Environ. Sci. Technol. 25:525–531.

Spadini, L., A. Manceau, P.W. Schindler, and L. Charlet. 1994. Structure and stability of Cd^{2+} surface complexes on ferric oxides: I. Results from EXAFS spectroscopy. J. Colloid Interface Sci. 168:73–86.

Sposito, G. 1983. On the surface complexation model of the oxide-aqueous solution interface. J. Colloid Interface Sci. 91:329–340.

Sposito, G., J.C.M. de Wit, and R.H. Neal. 1988. Selenite adsorption on alluvial soils: III. Chemical modeling. Soil Sci. Soc. Am. J. 52:947–950.

Sprycha, R. 1989a. Electrical double layer at alumina/electrolyte interface: I. Surface charge and zeta potential. J. Colloid Interface Sci. 127:1–11.

Sprycha, R. 1989b. Electrical double layer at alumina/electrolyte interface: II. Adsorption of supporting electrolyte ions. J. Colloid Interface Sci. 127:12–25.

Staley, G.B., G.P. Turi, and D.L. Schreiber. 1979. Radionuclide migration from low-level waste: A generic overview. p. 1041–1072. *In* M.W. Carter, A.A. Moghissi, and B. Kahn (ed.) Management of low-level radioactive waste. Pergamon Press, New York.

Stollenwerk, K.G. 1994. Geochemical interactions between constituents in acidic groundwater and alluvium in an aquifer near Globe, Arizona. Appl. Geochem. 9:353–369.

Stollenwerk, K.G. 1995. Modeling the effects of variable groundwater chemistry on adsorption of molybdate. Water Resour. Res. 31:347–357.

Stollenwerk, K.G. 1998. Molybdate transport in a chemically complex aquifer: Field measurements compared with solute-transport model predictions. Water Resour. Res. 34:2727–2740.

Strawn, D.G., A.M. Scheidegger, and D.L. Sparks. 1998. Kinetics and mechanisms of Pb(II) sorption and desorption at the aluminum oxide–water interface. Environ. Sci. Technol. 32:2596–2601.

Strawn, D.G., and D.L. Sparks. 1999. The use of XAFS to distinguish between

inner- and outer-sphere lead adsorption complexes on montmorillonite. J. Colloid Interface Sci. 21:257–269.
Streck, T., and J. Ritcher. 1997. Heavy metal displacement in a sandy soil at the field scale: 2. Modeling. J. Environ. Qual. 26:56–62.
Strenge, D.L., and S.R. Peterson. 1989. Chemical data bases for multimedia environmental pollutant assessment system (MEPAS), version 1. PNL-7145 Pacific Northwest Laboratory, Richland, WA.
Stumm, W., R. Kummert, and L.M. Sigg. 1980. A ligand exchange model for the adsorption of inorganic and organic ligands at hydrous oxide interfaces. Croat. Chem. Acta 53:291–312.
Su, C., and D.L. Suarez. 1995. Coordination of adsorbed boron: A FTIR spectroscopic study. Environ. Sci. Technol. 29:302–311.
Su, C., and D.L. Suarez. 1997. In situ infrared speciation of adsorbed carbonate on aluminum and iron oxides. Clays Clay Miner. 45:814–825.
Su, C., and D.L. Suarez. 2000. Selenate and selenite sorption on iron oxides: An infrared and electrophoretic study. Soil Sci. Soc. Am. J. 64:101–111.
Suarez, D.L., S. Goldberg, and C. Su. 1999. Evaluation of oxyanion adsorption mechanisms on oxides using FTIR spectroscopy and electrophoretic mobility. Am. Chem. Soc. Symp. Ser. 715:136–178.
Suarez, D.L., and J. Simunek. 1997. UNSATCHEM: Unsaturated water and solute transport model with equilibrium and kinetic chemistry. Soil Sci. Soc. Am. J. 61:1633–1646.
Sverjensky, D.A. 1993. Physical surface-complexation models for sorption at the mineral–water interface. Nature 364:776–780.
Sverjensky, D.A. 1994. Zero-point-of-charge prediction from crystal chemistry and solvation theory. Geochim. Cosmochim. Acta 58:3123–3129.
Sverjensky, D.A. 2001. Interpretation and prediction of triple-layer model capacitances and the structure of the oxide–electrolyte–water interface. Geochim. Cosmochim. Acta 65:3642–3655.
Sverjensky, D.A. 2003. Standard states for the activities of mineral surface sites and species. Geochim. Cosmochim. Acta 67:17–28.
Sverjensky, D.A., and N. Sahai. 1996. Theoretical prediction of single-site surface-protonation equilibrium constants for oxides and silicates in water. Geochim. Cosmochim. Acta 60:3773–3797.
Sylwester, E.R., E.A. Hudson, and P.G. Allen. 2000. The structure of uranium(VI) sorption complexes on silica, alumina, and montmorillonite. Geochim. Cosmochim. Acta 64:2431–2438.
Tejedor-Tejedor, M.L., and M.A. Anderson. 1990. Protonation of phosphate on the surface of goethite as studied by CIR-FTIR and electrophoretic mobility. Langmuir 6:602–611.
Thibault, D.H., M.I. Sheppard, and P.A. Smith. 1990. A critical compilation and review of default soil solid/liquid partition coefficients, K_d, for use in environmental assessments. AECL-100125. Atomic Energy of Canada, Whiteshell Nuclear Research Establishment.
Thomas, K. 1987. Summary of sorption measurements performed with Yucca Mountain, Nevada, tuff samples and water from Well J-13. LA-10960-MS. Los Alamos National Laboratory, Los Alamos, NM.
Thompson, H.A., G.A. Parks, and G.E. Brown. 1999. Dynamic interactions of dissolution, surface adsorption, and precipitation in an aging cobalt(II)–clay–water system. Geochim. Cosmochim. Acta 63:1767–1779.
Towle, S.N., J.R. Bargar, G.E. Brown, and G.A. Parks. 1997a. Surface precipitation of Co(II)(aq) on Al_2O_3. J. Colloid Interface Sci. 187:62–82.
Towle, S.N., J.R. Bargar, G.E. Brown, and G.A. Parks. 1999a. Sorption of Co(II) on metal oxide surfaces: II. Identification of specific binding sites of Co(II)(aq) adsorption sites on the (0001) and (1102) surfaces of α-Al_2O_3 by grazing-incidence XAFS spectroscopy. J. Colloid Interface Sci. 217:312–321.
Towle, S.N., J.R. Bargar, P. Persson, G.E. Brown, and G.A. Parks. 1997b. Surface precipitation in the Co(II)/Al_2O_3 system. p. 237–242. *In* J.A. Voigt, T.E. Wood, B.C. Bunker, W.H. Casey, and L.J. Crossey (ed.) Aqueous chemistry and geochemistry of oxides, oxyhydroxides, and related materials. Materials Research Society, San Francisco, CA.
Towle, S.N., G.E. Brown, and G.A. Parks. 1999b. Sorption of Co(II) on metal oxide surfaces. I. Identification of specific binding sites of Co(II) on (110) and (001) surfaces of TiO_2 (rutile) by grazing-incidence XAFS spectroscopy. J. Colloid Interface Sci. 217:299–311.
Trainor, T.P., G.E. Brown, and G.A. Parks. 2000. Adsorption and precipitation of aqueous Zn(II) on alumina powders. J. Colloid Interface Sci. 231:359–372.
Trivedi, P., L. Axe, and T.A. Tyson. 2001a. An analysis of zinc sorption to amorphous versus crystalline iron oxides using XAS. J. Colloid Interface Sci. 244:230–238.
Trivedi, P., L. Axe, and T.A. Tyson. 2001b. XAS studies of Ni and Zn adsorbed to hydrous manganese oxide. Environ. Sci. Technol. 35:4515–4521.
Trivedi, P., J.A. Dyer, and D.L. Sparks. 2003. Lead sorption onto ferrihydrite: 1. A macroscopic and spectroscopic assessment. Environ. Sci. Technol. 37:908–914.
Turner, D.R. 1993. Mechanistic approaches to radionuclide sorption modeling. CNWRA 93-019. Center for Nuclear Waste Regulatory Analyses, San Antonio, TX.
Turner, D.R. 1995. A uniform approach to surface complexation modeling of radionuclide sorption. CNWRA 95-001. Center for Nuclear Waste Regulatory Analyses, San Antonio, TX.
Turner, D.R., F.P. Bertetti, and R.T. Pabalan. 2002. Role of radionuclide sorption in high-level waste performance assessment: Approaches for the abstraction of detailed models. p. 211–252. *In* P.-C. Zhang and P.V. Brady (ed.) Geochemistry of soil radionuclides. SSSA Special Publ. 59. SSSA, Madison, WI.
Turner, D.R., and R.T. Pabalan. 1999. Abstraction of mechanistic sorption model results for performance assessment calculations at Yucca Mountain, Nevada. Waste Manage. 19:375–388.
USEPA. 1999a. Diffuse-layer sorption reactions for use in MINTEQA2 for HWIR metals and metalloids. EPA, National Exposure Research Laboratory, Ecosystems Research Division, Athens, GA.
USEPA. 1999b. MINTEQA2/PRODEFA2: A geochemical assessment model for environmental systems: User manual supplement for version 4.0. EPA, National Exposure Research Laboratory, Ecosystems Research Division, Athens, GA.
USEPA. 1999c. Understanding variation in partition coefficient, K_d, values. Vol. 1. The K_d model, methods of measurement, and application of chemical reaction codes. EPA 402-R-99-004A. USEPA, Washington, DC.
USEPA. 1999d. Understanding variation in partition coefficient, K_d, values. Vol. 2. Review of geochemistry and available K_d values for cadmium, cesium, chromium, lead, plutonium, radon, strontium, thorium, tritium (^3H), and uranium. EPA 402-R-99-004B. USEPA, Washington, DC.
USEPA. 2002. Understanding variation in partition coefficient, K_d, values, Vol. 3. Review of geochemistry and available K_d values for americium, arsenic, curium, iodine, neptunium, radium, and technetium. EPA 402-R-99-004C. USEPA, Washington, DC.
U.S. Nuclear Regulatory Commission. 1980. Final generic environmental impact statement on uranium milling. Vol. 1–3. G-V. NUREG-0706. Office of Nuclear Material Safety and Safeguards, U.S. Nuclear Regulatory Commission, Washington, DC.
Vandergraaf, T.T., K.V. Ticknor, and T.W. Melnyk. 1992. The selection and use of a sorption database for the geosphere model in the Canadian Nuclear Fuel Waste Management Program. p. 81–120. *In* Radionuclide sorption from the safety evaluation perspective. Proc. of a Nuclear Energy Agency Workshop, Interlaken, Switzerland. 16–18 October 1991. OECD, Paris, France.
van der Lee, J., and C. Lomenech. 2004. Towards a common thermodynamic database for speciation models. Radiochim. Acta 92:811–818.
van der Zee, S.E.A.T.M., and W.H. van Riemsdijk. 1987. Transport of reactive solute in spatially-variable soil systems. Water Resour. Res. 23:2059–2069.
Vaughan, P.J., P.J. Shouse, S. Goldberg, D.L. Suarez, and J.E. Ayars. 2004. Boron transport within an agricultural field: Uniform flow versus mobile-immobile water model simulations. Soil Sci. 169:401–412.
Venema, P., T. Hiemstra, and W.H. van Riemsdijk. 1996. Multisite adsorption of cadmium on goethite. J. Colloid Interface Sci. 183:515–527.
Villalobos, M., and J.O. Leckie. 2001. Surface complexation modeling and FTIR study of carbonate adsorption to goethite. J. Colloid Interface Sci. 235:15–32.
von Gunten, H.R., G. Karametaxas, U. Krahenbuhl, M. Kuslys, R. Giovanoli, E. Hoehn, and R. Keil. 1991. Seasonal biogeochemical cycles in riverborne groundwater. Geochim. Cosmochim. Acta 55:3597–3609.
Waite, T.D., J.A. Davis, B.R. Fenton, and T.E. Payne. 2000. Approaches to modeling uranium (VI) adsorption on natural mineral assemblages. Radiochim. Acta 88:687–693.
Waite, T.D., J.A. Davis, T.E. Payne, G.A. Waychunas, and N. Xu. 1994. Uranium (VI) adsorption to ferrihydrite: Application of a surface complexation

model. Geochim. Cosmochim. Acta 58:5465–5478.
Waychunas, G.A., C.C. Fuller, and J.A. Davis. 2002. Surface complexation and precipitate geometry for aqueous Zn(II) sorption on ferrihydrite: I. X-ray absorption extended fine structure spectroscopic analysis. Geochim. Cosmochim. Acta 66:1119–1137.
Waychunas, G.A., C.C. Fuller, J.A. Davis, and J.J. Rehr. 2003. Surface complexation and precipitate geometry for aqueous Zn(II) sorption on ferrihydrite: II. XANES analysis and simulation. Geochim. Cosmochim. Acta 67:1031-1043.
Waychunas, G.A., B.A. Rea, C.C. Fuller, and J.A. Davis. 1993. Surface chemistry of ferrihydrite: Part 1. EXAFS studies of the geometry of coprecipitated and adsorbed arsenate. Geochim. Cosmochim. Acta 57:2251–2269.
Weesner, F.J., and W.F. Bleam. 1997. X-ray absorption and EPR spectroscopic characterization of adsorbed copper(II) complexes at the boehmite (AlOOH) surface. J. Colloid Interface Sci. 196:79–86.
Weesner, F.J., and W.F. Bleam. 1998. Binding characteristics of Pb^{2+} on anion-modified and pristine hydrous oxide surfaces studied by electrophoretic mobility and X-ray absorption spectroscopy. J. Colloid Interface Sci. 205:380–389.
Whelan, G., J.P. McDonald, and C. Sato. 1996. Multimedia environmental pollutant assessment system (MEPAS): Groundwater pathway formulations. PNNL-10907. Pacific Northwest National Laboratory, Richland, WA.
Wijnja, H., and C.P. Schulthess. 1999. ATR-FTIR and DRIFT spectroscopy of carbonate species at the aged γ-Al_2O_3/water interface. Spectrochim. Acta A Mol. Biomol. Spectrosc. 55:861–872.
Wijnja, H., and C.P. Schulthess. 2000. Vibrational spectroscopy study of selenate and sulfate adsorption mechanisms on Fe and Al (hydr)oxide surfaces. J. Colloid Interface Sci. 229:286–297.
Wijnja, H., and C.P. Schulthess. 2001. Carbonate adsorption mechanism on goethite studied with ATR-FTIR, DRIFT and proton coadsorption measurements. Soil Sci. Soc. Am. J. 65:324–330.
Yu, C., C. Loureiro, J.-J. Cheng, L.G. Jones, Y.Y. Wang, Y.P. Cia, and E. Faillace. 1993b. Data collection handbook to support modeling the impacts of radioactive material in soil. ANL/EAIS-8. Argonne National Laboratory, Argonne, IL.
Yu, C., A.J. Zielen, J.-J. Cheng, Y.C. Yuan, L.G. Jones, D.J. LePoire, Y.Y. Wang, C. Loureiro, E. Gnanapragasam, E. Faillace, A. Wallo, W.A. Williams, and H. Peterson. 1993a. Manual for implementing residual radioactive material guidelines using RESRAD, version 5.0. ANL/EAD/LD-2. Argonne National Laboratory, Argonne, IL.
Zachara, J.M., P.L. Gassman, S.C. Smith, and D. Taylor. 1995. Oxidation and adsorption of Co(II)$EDTA^{2-}$ complexes in subsurface materials with iron and manganese oxide grain coatings. Geochim. Cosmochim. Acta 59:4449–4463.
Zeltner, W.A., E.C. Yost, M.L. Machesky, M.L. Tejedor-Tejedor, and M.A. Anderson. 1986. Characterization of anion binding on goethite using titration calorimetry and cylindrical internal reflection–Fourier transform infrared spectroscopy. Am. Chem. Soc. Symp. Ser. 323:142–161.